Proteomic Analysis of High-CO_2-Inducible Extracellular Proteins in the Unicellular Green Alga, *Chlamydomonas reinhardtii*

Masato Baba, Iwane Suzuki and Yoshihiro Shiraiwa*

Graduate School of Life and Environmental Sciences, 1-1-1 Tennodai, University of Tsukuba, Tsukuba, 305-8572 Japan

*Corresponding author: E-mail, emilhux@biol.tsukuba.ac.jp; Fax, +81-29-853-6614

The unicellular green alga *Chlamydomonas reinhardtii* can acclimate to a wide range of CO_2 concentrations through the regulation of a CO_2-concentrating mechanism (CCM). By proteomic analysis, here we identified the proteins which were specifically accumulated under high-CO_2 conditions in a cell wall-less strain of *C. reinhardtii* which releases extracellular matrices to the medium. When CO_2 concentration was elevated from the air-level to 3% during culture, the algal growth rate increased 1.5-fold and the composition of extracellular proteins, but not intracellular-soluble and -insoluble proteins, clearly changed. Proteomic analysis data showed that the levels of 22 among 129 extracellular proteins increased for 1 and 3 days and such multiple high-CO_2-inducible proteins include gametogenesis-related proteins and hydroxyproline-rich-glycoproteins. However, we could not prove the induction of gametogenesis under high-CO_2 conditions, suggesting that the inductive signal might be incomplete, not strong enough, or only high-CO_2 conditions might be not sufficient for proceeding cell stage to the formation of sexually active gamates. In any case, those gametogenesis-related proteins and/or hydroxyproline-rich-glycoproteins may take novel roles outside the cell under high-CO_2 conditions.

Keywords: *Chlamydomonas reinhardtii* • extracellular proteins • gametogenesis • high-CO_2-inducible protein • high-CO_2-acclimation • proteomics

Abbreviations: CAH, carbonic anhydrase; CCM, CO_2-concentrating mechanism; DIC, dissolved inorganic carbon; emPAI, exponentially modified Protein Abundance Index; FAP, flagellar-associated protein; GAS, gamete-specific; GP, glycoprotein; H43/FEA1, high-CO_2-inducible 43 kDa protein/Fe-assimilation 1; HRGP, hydroxyproline-rich glycoprotein; ISG, inversion-specific glycoprotein; MMP, matrix metalloproteinase; MS, mass spectrometry; NSG, nitrogen-starved gametogenesis; PHC, pherophorin; SDS-PAGE, sodium dodecyl sulfate-polyacrylamide gel electrophoresis.

Introduction

Aquatic photosynthetic organisms such as microalgae and cyanobacteria have an ability to acclimate to a broad range of CO_2 concentrations. CO_2 is the substrate of photosynthetic carbon fixation and therefore the rate of CO_2 supply is a key factor for efficient photosynthetic reactions. The process of dissolving atmospheric CO_2 into water, the subsequent processes of equilibration of dissolved CO_2, bicarbonate, and carbonate, and the diffusion of those dissolved inorganic carbons (DIC) to cells and the CO_2 fixation site in chloroplasts are extremely slow physical and chemical processes, compared to other enzymatic reactions in photosynthesis. Furthermore, these processes are strongly affected by various environmental factors such as pH, temperature, and salinity. The atmospheric and oceanic CO_2 concentrations decreased markedly during certain geological periods and there have been several incidences of minor fluctuations in CO_2. This would suggest that photosynthetic organisms have developed special mechanisms for DIC utilization and for metabolic pathways to adapt and acclimate to changes in CO_2 concentration (*e.g.*, Badger 1987; Falkowski and Raven 2007). However, some properties of a CO_2-fixing enzyme ribulose-1, 5-bisphosphate carboxylase/oxygenase (Rubisco) are less developed; *e.g.*, the relative specificity of Rubisco to CO_2/O_2 and an affinity of Rubisco to CO_2 (*e.g.*, Falkowski and Raven 2007).

Microalgae induce a CO_2-concentrating mechanism (CCM) that facilitates the utilization of DIC through the *de novo* synthesis of inorganic carbon transporters and carbonic anhydrases (CAHs) when cells are exposed to air-level CO_2 conditions (*i.e.*, ca. 10 μM CO_2 in the medium) (Badger et al. 1980; Aizawa and Miyachi 1986; Kaplan and Reinhold 1999; Miyachi et al. 2003; Badger et al. 2006; Raven et al. 2008; Spalding 2008; Moroney and Ynalvez 2007; Yamano and Fukuzawa 2009). The induction of CCM

63 is immediately suppressed and its activity decreases gradually under high-CO_2 conditions
64 (for review, see Miyachi et al. 2003).

65 In contrast to the low-CO_2-inducible phenomena, high-CO_2-inducible and
66 low-CO_2-suppressive phenomena have not been well-studied. Even though some
67 microalgae and cyanobacteria are able to grow under extremely high-CO_2 (*e.g.*, 40–100%
68 CO_2), in general, they are susceptible to extremely high-CO_2 conditions (for review, see
69 Miyachi et al. 2003). The effects of extremely high-CO_2 on cellular responses have been
70 studied extensively in the high-CO_2-tolerant marine chlorophyte *Chlorococcum littoralle*.
71 When cells were transferred to extremely high-CO_2 conditions, photosynthetic activity
72 was spontaneously decreased by chloroplastic and cytosolic acidifications. Then *C.*
73 *littoralle* recovers to acclimate via state transition for protecting photosystems from
74 damage (Iwasaki et al. 1998; Sasaki et al. 1998; Satoh et al. 2001, 2002, 2004). However,
75 the half-saturation concentration of CO_2 of high-CO_2-acclimated cells to be adequate for
76 changing cellular characteristics has been reported to be 0.5% in a unicellular green alga
77 *Chlorella kessleri* 211-11h (formerly *C. vulgaris*11h; Shiraiwa and Miyachi 1985).
78 Accordingly, the cellular acclimation to high-CO_2 conditions was suggested to be
79 different from that to extremely high-CO_2.

80 A unicellular green alga, *Chlamydomonas reinhardtii* has been used widely as a model
81 organism for photosynthesis research. It lives in aquatic environments and even in soil
82 where CO_2 concentration change drastically between the atmospheric level and ≥10%
83 (v/v) (for review, see Buyanovsky and Wagner 1983; Stolzy 1974). To survive in such
84 habitats, this alga needs to acclimate and adapt to high-CO_2 conditions rather than
85 low-CO_2. We previously demonstrated that a change in CO_2 concentration from air-level
86 to 3% CO_2 in air induces a dramatic change in the composition of extracellular proteins in

87 *C. reinhardtii* (Kobayashi et al. 1997; Hanawa et al. 2004; Hanawa et al. 2007). We found
88 that carbonic anhydrase 1 (CAH1), the most abundant extracellular protein in the
89 low-CO_2 cells, is replaced by high-CO_2-inducible 43 kDa protein/Fe-assimilation 1
90 (H43/FEA1), a function-unknown protein, when cells were exposed to high-CO_2
91 conditions (Allen et al. 2007; Baba et al. 2011; Hanawa et al. 2004, 2007; Kobayashi et al.
92 1997). Previous studies demonstrate that the expression of H43/FEA1 is separately
93 regulated by CO_2 and iron concentrations via independent *cis*-elements (Allen et al. 2007;
94 Hanawa et al. 2007; Fei et al. 2009; Baba et al. 2011). It has been suggested that the
95 homologous genes of *H43/Fea1* can be found in the genomic sequences of the
96 chlorophytes *Scenedesmus obliquus*, *Volvox carteri*, and *C. littorale* and the
97 dinoflagellate *Heterocapsa triquerta* (Allen et al. 2007). A homolog of *H43/Fea1* in *C.*
98 *littorale*, *Hcr1*, had been identified previously as a high-CO_2-responsive gene (Sasaki et
99 al. 1998). These results suggest that the orthologs of *H43/Fea1* may play a role in
100 high-CO_2 acclimation in these algae. In addition to H43/FEA1, carbonic anhydrase 2
101 (CAH2) (Fujiwara et al. 1996) and Rhesus1 (Soupene et al. 2004) have also been reported
102 as high-CO_2-inducible proteins in *C. reinhardtii*; however, their physiological functions
103 have not yet been revealed.

104 These findings of high-CO_2-inducible proteins indicate that *C. reinhardtii* cells can
105 actively acclimate to high-CO_2 conditions by not only reducing low-CO_2-inducible CCM
106 and CAH activities, but also through a high-CO_2-inducible mechanism. To understand the
107 details of such acclimation, we conducted an exhaustive search of proteins using
108 genome-based liquid chromatography-mass spectrometry (LC-MS) methods to
109 characterize the entire profile involved in the cellular response to high-CO_2 conditions in
110 *C. reinhardtii*.

111

112 **Results**

113 **Effect of high-CO_2 on cell growth and protein content**

114 We used the cell wall-less strain *C. reinhardtii* CC-400 cw-15 mt^+ in this study because
115 the strain largely releases extracellular matrices, including periplasmic proteins, into the
116 medium (Hanawa et al. 2007). We accurately called such proteins released to the medium
117 as extracellular proteins of which major components are periplasmic proteins.

118 The logarithmic growth phase of CC-400 was maintained only for about 24 h in a
119 batch culture, irrespective of CO_2 concentrations (Fig. 1A). The growth rate μ (d^{-1}) and
120 average doubling time (h; shown in parenthesis), were 1.8 (8.95), 2.2 (7.60), and 2.4
121 (6.81) for air-grown cells transferred to air (Air), air-grown cells transferred to 3% CO_2 in
122 air (Air to CO_2), and 3% CO_2-grown cells transferred to 3% CO_2 in air (CO_2), respectively
123 (Fig. 1B). When the growth reached the linear growth phase by increasing cell
124 concentration, the cell growth became especially slow under air (Fig. 1B).

125 To avoid such growth limitation, a semi-continuous culture method in which a cell
126 suspension was diluted once per day with fresh medium was introduced for preparing
127 samples for proteomic analysis (Fig. 2). The experiments were repeated three times and
128 data presented here are average values of them. Algal samples acclimated to low- and
129 high-CO_2 conditions were provided for protein analysis, as follows: cells grown under
130 ambient atmospheric air, namely CO_2-limiting conditions (Air), cells grown for 1 day
131 under high-CO_2 conditions (CO_2-1d), and cells grown for 3 days under high-CO_2
132 conditions (CO_2-3d) (Fig. 2A). The growth rates μ (d^{-1}) and average doubling times (h) in
133 parenthesis were 1.81 ± 0.06 (9.19 ± 0.32), 2.7 ± 0.23 (6.19 ± 0.55), and 2.78 ± 0.04
134 (5.98 ± 0.09) under Air, CO_2-1d, and CO_2-3d, respectively (Fig. 2B). The logarithmic

135 growth rate (μ) of CO_2-3d was 1.5-fold higher than that of Air. The amount of proteins
136 released into the medium was slightly greater in CO_2-3d cells than in Air cells (Fig. 2C).
137 The fluorescent gel images of extracellular proteins separated by sodium dodecyl
138 sulfate-polyacrylamide gel electrophoresis (SDS-PAGE) clearly showed the induction of
139 CAH1 and H43/FEA1, which are known to be low- and high-CO_2-inducible markers, in
140 air-acclimated cells and high-CO_2 acclimated cells, respectively (Fig. 2D). Such different
141 profiles of CAH1 and H43/FEA1 demonstrate that the cells were fully acclimated to low-
142 and high-CO_2 conditions, respectively.

143 Intracellular-soluble and -insoluble fractions were applied separately to 2D-gel
144 analysis of low- and high-CO_2-acclimated cells. The major proteins were Rubisco (Fig.
145 S1A, B) and the photosystem-associated proteins disturbed clear separation of proteins in
146 the intracellular-soluble and intracellular-insoluble fractions, respectively, but no clear
147 difference was observed between the low- and high-CO_2-acclimated cells (Fig. S1C). We
148 only found significant changes in the profile of extracellular proteins and therefore we
149 focused on these profiles in subsequent analyses.

150 One-dimensional SDS-PAGE was sufficient to separate the extracellular proteins for
151 mass spectrometric analysis. Consequently, we identified 89, 69, and 98 proteins from
152 culture media of Air, CO_2-1d, and CO_2-3d cells, corresponding to the samples presented
153 in Fig. 2A (Table S1). The total number of proteins, identified at least once in triplicate
154 experiments with a MASCOT score >50, was 129. The data are presented together with
155 the exponentially modified Protein Abundance Index (emPAI) because the emPAI is
156 useful for estimating the absolute amount of protein (Ishihama et al. 2005). According to
157 the SignalP 3.0 server prediction, number (percent of total proteins) of proteins predicted
158 to be secretory was 32 (36.0%), 33 (47.8%), and 40 (40.8%) in Air, CO_2-1d cells, and

159 CO_2-3d cells, respectively, where total number was 43 (33.3%) (Fig. 3). On the other
160 hand, the percentage of total putative secretory proteins calculated on the basis of protein
161 amounts was 46.5%, 63.0%, and 65.9% in Air, CO_2-1d, and CO_2-3d cells, respectively,
162 indicating that high-CO_2-acclimated cells secreted 1.4-fold more proteins than did
163 low-CO_2-acclimated cells. These proteins were annotated based on the results of BlastX
164 analyses and are listed separately up to 20 in order of their amounts in Air, CO_2-1d, and
165 CO_2-3d cells in Tables 1–3 and Fig. 4. Proteins highly induced under high-CO_2 conditions
166 were renamed as high-CO_2-inducible proteins (HCI) (Table S1). Other extracellular
167 proteins that had no name were designated extracellular proteins (EXC).
168
169 **Highly induced extracellular proteins in air-acclimated cells**
170 Out of 89 proteins, 31 were identified in Air cells tested in triplicate (Table S1).
171 Among them, the ratios of the amounts (mol%) of CAH1 and
172 glyceraldehyde-3-phosphate dehydrogenase 3 (GAP3) in Air to CO_2-3d cells
173 (Air/CO_2-3d) were 5.85 and 5.25 (p <0.05), respectively (Table 1, Fig. 4). CAH1 was the
174 most abundant protein in Air cells, amounting to 10.11 ± 2.84% of the total extracellular
175 proteins. CAH1 localizes in the periplasmic space (Kimpel et al., 1983, Coleman et al.,
176 1984, Yang et al., 1985, Fukuzawa et al., 1990). Although CAH2, generally known as a
177 high-CO_2-inducible protein, was identified as a low-CO_2-inducible protein by database,
178 the identification contains uncertainty because CAH2 has a similar amino acid sequence
179 to CAH1 and very low protein content (data not shown). Therefore, we hereby described
180 it as CAH1/CAH2 (Table 1, Fig. 4). The location of GAP3 predicted by SignalP was in
181 the cytoplasm, but this protein has also been reported in flagella proteome (Pazour et al.,
182 2005), suggesting that it is a multi-protein. As such, the annotation of proteins contained

183 some less-reliable cases.

184 The levels of other proteins of low content were not significantly different between Air
185 and CO_2-3d cells.

186

187 **Highly induced extracellular proteins in 1-day high-CO_2-acclimated cells**

188 Similarly, 44 of 69 proteins were identified in triplicate experiments in CO_2-1d cells
189 (Table S1). Among them, the amounts of seven proteins (H43/FEA1, two
190 nitrogen-starved gametogenesis [NSG] family proteins [HCI1 and HCI2], two
191 glycoproteins [GP1 and FAP102], and two inversion-specific glycoproteins [ISG-C1 and
192 ISG-C4]) were significantly higher (p <0.05) in CO_2-1d cells than in Air cells (Table 2,
193 Fig. 4). H43/FEA1 was the most abundant protein, accounting for 22.09 ± 8.16 (mol%) of
194 the total extracellular proteins in CO_2-1d cells. The ratios of the amount (mol%) of
195 proteins in CO_2-1d to Air cells (CO_2-1d/Air) were 3.66, 3.57, 2.26, and 2.07 for
196 H43/FEA1, ISG-C1 (similar to *V. carteri* ISG and *C. reinhardtii* VSP-3), FAP102 (similar
197 to GP3), and HCI1 (similar to NSG1), respectively (Fig. 4).

198

199 **Highly induced extracellular proteins in 3-day high-CO_2-acclimated cells**

200 Of 98 proteins, 41 were identified in triplicate experiments in all CO_2-3d cells (Table
201 S1). Among them, the amounts (mol%) of eight proteins (H43/FEA1, three NSG family
202 proteins [FAP212, HCI2, and HCI3], two GPs [FAP102 and HCI4], and two ISGs
203 [ISG-C1 and ISG-C2]) were significantly higher in CO_2-3d cells than in Air cells (p
204 <0.05) (Table 3, Fig. 4). H43/FEA1 was the most abundant protein, amounting to
205 26.01 ± 4.30 (mol%) of total extracellular proteins in CO_2-3d cells (Table 3, Fig. 4). The
206 ratios of the amount of proteins in CO_2-3d to Air cells (CO_2-3d/Air) were 4.36, 4.31, 3.03,

and 2.48 in ISG-C1, H43/FEA1, HCI3 (similar to NSG1), and FAP102, respectively. ISG-C2 (similar to *V. carteri* ISG and *C. reinhardtii* VSP-3) was not observed in Air cells, but was observed at significant levels in CO_2-3d cells in triplicate. Likewise, HCI4 (similar to GP3) was identified in CO_2-3d cells. HCI3 and FAP 212 (similar to NSG1) were already found in CO_2-1d cells in triplicate and their amounts were not significantly higher than those in Air cells (Table 3, Fig. 4). On the other hand, ISG-C2 and HCI4 were only found in two of the triplicate samples of CO_2-1d cells (Table S1). Consistent with the CO_2-1d cell results, HCI1, GP1, and ISG-C1 were identified again in CO_2-3d cells, but their amounts were not significantly higher than those in Air cells (Table 3, Fig. 4).

Mating efficiency of high-CO_2 cells

According to the proteomic analysis data suggesting that gametogenesis might be induced under high-CO_2 conditions, we examined the mating efficiency under the same culture conditions. For the purpose we used high-mating strains of *C. reinhardtii* strains CC-620 and CC-621 since the cell wall-less strain generally is known to show low mating efficiency. As a result, when those were grown under high-CO_2, both strains did not show mating profile whereas gamete formation was triggered by nitrogen-depletion and the gamates showed normal mating profile (Fig. 5). A mating efficiency of gamates induced by nitrogen-depletion was approximately 75% (data not shown).

Discussion

General features of high-CO_2-acclimated cells

The major component of the cellular response to limited CO_2 is the activation of CCM, which is reversibly inactivated under high-CO_2 conditions (for review, see Aizawa and

231 Miyachi 1986, Badger 1987, Kaplan and Reinhold 1999, Miyachi et al. 2003). In this
232 study, we analyzed high-CO_2-inducible proteins in *C. reinhardtii* by proteomic analysis.
233 Although we did not find any significant changes in intracellular proteins after the
234 transfer of cells from air to 3% CO_2 in air (Fig. S1), we observed remarkable changes in
235 the amount and composition of extracellular proteins (Figs. 2D, 4 and Table S1). The
236 algal growth rate and the amount of total proteins increased by only 1.5-fold, even when
237 the CO_2 concentration increased ca. 75-fold from ca. 0.04 to 3% in a wall-less mutant of
238 *C. reinhardtti* CC-400 (Fig. 1). These results indicate that air-acclimated cells could grow
239 quickly, at a rate close to the maximum growth potential, and this may be due to the
240 organism having established a mechanism for the efficient utilization of ambient CO_2
241 such as CCM. The big difference in growth rates between Air- and 3% CO_2-acclimated
242 cells was obvious during the linear growth phase and this seems to be a reason why
243 air-grown cultures take longer to attain a high algal density.
244
245 **Low- and high-CO_2-inducible extracellular proteins**
246 The induction of CAH1 and H43/FEA1, which are known as low- and
247 high-CO_2-inducible proteins, respectively, demonstrated that our proteomic analysis was
248 performed under adequate conditions (Fig. 4). Interestingly, GAP3 was dominantly
249 induced under low-CO_2 (Table 1, Fig. 4). GAP3 has been implicated in flagellar activity
250 (Pazour et al. 2005). GAP activity has been shown to correlate with cell motility in
251 *Dunaliella salina* (Jia et al. 2009), implying that decreased CO_2 availability may
252 stimulate cell motility.
253 We also found that two mastigoneme-like proteins, MST1 (a flagellar component;
254 Pazour et al. 2005) and HCI5, were induced under high-CO_2 conditions (Table S1). We

255 also found some function-unknown flagellar associated proteins, or FAPs (Pazour et al.
256 2005), although the expression pattern of each FAP depended on the levels of CO_2 (*e.g.*,
257 FAP211 and FAP102). In our study, FAPs were found in the excreted protein fraction and
258 therefore we cannot exclude the possibility that the annotation of FAPs contains some
259 uncertainty. Consequently, our results suggest that a high-CO_2 signal may induce the
260 expression of each flagellar component, but the detailed mechanism needs to be analyzed.
261 Some NSG family proteins were specifically induced under high-CO_2 (Table 3, Fig. 4).
262 NSG family genes were previously identified in synchronized early G1 cells of *C.*
263 *reinhardtii* grown in nitrogen-free medium (Abe et al. 2004).
264 We found that GP and ISG family proteins were significantly induced under high-CO_2
265 conditions (Table 3, Fig. 4). GP has been isolated from major outer layers of cell walls
266 (W6 and W4) using sodium perchlorate or other chaotropes (Goodenough et al. 1986).
267 Although GPs are thought to be ones of major components of cell wall, the expression of
268 the proteins are rather enhanced in the cell wall-less mutant. Lack of cell wall might
269 release a feedback control by products. ISG is an extracellular glycoprotein of *V. carteri*
270 that may be synthesized for only a few minutes in inverting embryos and sperm cell
271 packets and is thought to be involved in the early processes of extracellular matrix
272 biogenesis (Ertl et al. 1992). Both GP and ISG were classified as hydroxyproline-rich
273 glycoproteins (HRGPs) together with pherophorin (PHC), gamete-specific (GAS) protein,
274 and sexual agglutinin with a shared origin (Adair 1985). PHC, a common protein in
275 volvocales (Hallmann 2006), is abundant in the extracellular matrix and some of them
276 have been reported to be strongly induced by sex inducers that trigger sexual
277 development as well as by mechanical wounding (Hallmann 2006). GAS proteins are
278 related to PHCs (Hallmann 2006). Transcripts for GAS28, GAS30, and GAS31

accumulate in the late phase of gametogenesis and in young zygotes (Hoffmann and Beck 2005). In our experiments, a GAS family protein (HCI6) and three PHC proteins (HCI7, HCI8, and PHC14) accumulated in cells grown under high-CO_2 conditions (Table S1). These findings suggest that high-CO_2 signals may induce HRGPs, which have been reported to be generally involved in sexual recognition of mating-type plus and minus gametes in the *Chlamydomonas* lineage (Lee et al. 2007).

Furthermore, we found that two matrix metalloproteinases (MMPs), MMP1 and HCI9, which are gamete-lytic enzymes, were induced under high-CO_2 conditions (Table S1). Gamete-lytic enzymes degrade cell walls during gametogenesis (Buchanan and Snell 1988; Kinoshita et al. 1992) and the MMP1 gene is induced during gametogenesis (Kubo et al. 2001). The expression of gamete-lytic enzymes is restricted under nitrogen-deficient conditions.

These proteomic results indicate that multiple extracellular HRGPs proteins, such as NSG, ISG, and GP proteins, together with PHC, GAS, and gamete-lytic enzymes (Table S1) are induced under high-CO_2 conditions. Among these proteins, NSG, GAS, and gamete-lytic enzymes are generally known to be induced during the gametogenetic process, which is triggered by nitrogen-depletion.

Gametogenesis-related proteins expressed under high-CO_2 conditions

Sears et al. (1980) previously reported that the vegetative cells of *C. reinhardtii* logarithmically grown in HS medium contained 6-10 μg N $(10^6 \text{ cells})^{-1}$. Daily increments of cells under Air, CO_2-1d, and, CO_2-3d were 2.4×10^6 5.2×10^6, 7.7×10^6, respectively, where cell densities were maintained less than 10^7 cells ml^{-1} by daily dilution in the present experiments (Fig. 2B). Thus the nitrogen consumption by cells under Air, CO_2-1d,

303 and, CO_2-3d can be estimated to be 14-24, 31-52, and 46-77 mg l^{-1} in a day. As HS
304 medium firstly contains 500 mg l^{-1} NH_4Cl (9.35 mM), the nitrogen contents can be
305 estimated to remain between 7.91-9.09 mM in any culture. In previous studies,
306 gametogenesis of *C. reinhardtii* was immediately and strongly inhibited by 7.5 mM
307 NH_4Cl (Beck and Acker 1992). Accordingly, the significant induction of NSG, GAS, and
308 gamete-lytic enzymes would be due to high-CO_2 conditions, and not to external
309 nitrogen-depletion (Table 3, Fig. 4).

310 Nitrogen-depletion is an important inducing factor for gametogenesis (Sager and
311 Granick 1954); however, Goodenough et al. (2007) reported that nitrogen-depletion is a
312 necessary but not essential process for activating the gametogenetic program in *C.*
313 *reinhardtii.* Because the gene expressions for gametogenesis started with a certain length
314 of lag phase after the depletion of nitrogen from the medium, the external nitrogen
315 concentration seems to be a triggering factor, but not a regulatory signal. In terrestrial
316 plants, carbon and nitrogen metabolism interact tightly with each other (for review, see
317 Reichi et al. 2006), and carbon–nitrogen ratio signaling plays an important role in
318 environmental responses (for review, see Zheng, 2009). Taking our results into
319 consideration, a particular carbon–nitrogen ratio, generated under high-CO_2 conditions or
320 nitrogen-depletion, is likely to act as a signal for gametogenesis.

321 Some interesting consistencies have been reported in proteins that facilitate DIC and
322 nitrogen utilization, although their induction mechanisms are different. LCIA (also
323 named NAR1.2), which is involved in chloroplast-located bicarbonate transport
324 (Duanmu et al. 2009), was identified as a low-CO_2-inducible gene by EST analysis and
325 was shown to be regulated by changes in CO_2 but not nitrogen availability (Miura et al.
326 2004). On the other hand, NAR1 genes are generally known to involve members of the

Formate/Nitrite Transporter (FNT) family (Rexach et al. 2000). In fact, LCIA-containing *Xenopus* oocytes display both low-affinity bicarbonate transport and high-affinity nitrite transport (Mariscal et al. 2006), suggesting that LCIA is involved not only in bicarbonate uptake but also nitrite uptake under low-CO_2 conditions; in other words, the suppression of LCIA by high-CO_2 may reduce nitrogen availability. In addition, the molecular structure of the high-affinity-bicarbonate transporter *cmpABCD* is very similar to the nitrate/nitrite transporter *nrtABCD* in *Synechococcus* sp. PCC7942, suggesting a close regulatory relationship between carbon and nitrogen assimilation (for review, see Badger and Price 2003). These data suggest the possibility that changes in CO_2 availability may also affect nitrogen availability.

However, we could not find any effect of high-CO_2 signal alone on mating (Fig. 5). This result suggest that high-CO_2 signal induced gametogenesis-related proteins but the signal was not strong enough or still missing some factors required for triggering mating. Otherwise, it may also be possible that the gametogenesis-related protein families and/or hydroxyproline-rich-glycoproteins play another role under high-CO_2 conditions.

The present results suggest that high-CO_2 may be associated with sexual differentiation, by participating in gametogenesis and the sexual program. For further, detailed analysis of the relationship between high-CO_2 and gametogenesis, whole-cell proteome analysis would be necessary. Targeted proteomics of whole *C. reinhardtii* established by Wienkoop et al. (2010) might be useful for such an analysis. Future works are needed to determine which factor is essential for triggering gametogenesis and mating, namely high-CO_2, nitrogen-depletion or C/N ratio alone or in combination. Our findings also provide important clues for understanding the behavior of this organism in the natural environment.

Materials and Methods

Strains and culture conditions

A cell wall-less strain of a unicellular green microalga, *C. reinhardtii* CC-400 cw-15 mt^+, was obtained from the Chlamydomonas Center at Duke University for use in proteomic analyses. A pair of high-mating strains of *C. reinhardtii*, CC-620 mt^+ and CC-621 mt^-, was obtained from Dr. Y. Hanawa, International Patent Organism Depositary (IPOD), National Institute of Advanced Industrial Science and Technology (AIST), Japan for use in mating analysis. Cells were grown at 25°C in Erlenmeyer flasks containing 500 ml of modified HS medium (Sueoka 1960) supplemented with 30 mM 3-(N-morpholino) propanesulfonic acid (MOPS)-NaOH (pH 6.8), and grown under continuous illumination at a photosynthetic photon flux density (PPFD) of 150 μmol m^{-2} s^{-1}. Cells grown for 3 days were transferred to either atmospheric air or high (3%)-CO_2 conditions, as described previously (Hanawa et al., 2007).

For proteomic analysis, cells were grown in a semi-continuous culture by diluting each cell suspension with fresh media once per day to maintain a logarithmic growth phase. The algal cells were grown under the bubbling of air (0.04% [v/v] CO_2) for several days to fully acclimate to low-CO_2. After harvesting to transfer to fresh medium, cells were washed three times with fresh media to remove a tiny amount of extracellular proteins on the cell surface. Then, the washed cells were transferred to a new culture under continuous bubbling of air enriched with 3% (v/v) CO_2 (Fig. 2A).

For mating analysis, gamates triggered by nitrogen-depletion were prepared under either high-CO_2 or nitrogen-free conditions in modified HS medium supplemented with 30 mM MOPS-NaOH (pH 6.8) but no NH_4Cl.

375

376 **Sample preparation**

377 Aliquots (150 ml) of cultures were withdrawn and centrifuged at 2,300 × *g* for 10 min at
378 4°C to separate culture media and algal cells. Then, 0.12 mg ml^{-1} of complete protease
379 inhibitor cocktail (Roche diagnostics, Basel, Switzerland) was added to the collected
380 culture medium. Tiny floating particles in the culture media were removed by filtration
381 through a cellulose acetate membrane (430624, 0.22 μm, Corning, Corning, NY) and the
382 filtrate was lyophilized. The extracellular proteins were dissolved in 2 ml H_2O and then
383 dialyzed against H_2O. The protein concentration was determined using a commercial
384 assay kit (Bio-Rad Laboratories, Hercules, CA).

385 To obtain intracellular-soluble and -insoluble fractions, cells were washed twice with
386 fresh modified HS medium at 4°C and suspended in 1/50 volume of disruption buffer
387 containing 50 mM piperazine-N,N'-bis(2-ethanesulfonic acid) (PIPES)-NaOH (pH 7.0),
388 5 mM ethylene diamine tetraacetic acid (EDTA), 5 mM ethylene glycol tetraacetic acid
389 (EGTA), 100 mM NaCl, 1 mM phenylmethylsulfonyl fluoride (PMSF), and 1.2 mg ml^{-1}
390 complete protein inhibitor cocktail. Then the cells were disrupted by sonication on ice
391 and centrifuged to remove cell debris. The resultant supernatants were ultracentrifuged
392 twice: first at 50,000 × *g* and then at 98,000 × *g* for 30 min each. The final supernatants
393 were collected as the soluble proteins. Both precipitates were combined and washed twice
394 with disruption buffer and then used to prepare the insoluble proteins.

395 The intracellular-soluble and -insoluble proteins were precipitated with four volumes
396 of cold acetone. The precipitated soluble proteins were suspended in 8.5 M urea, 0.2%
397 (w/v) SDS, 2% (v/v) Triton X-100, 65 mM dithiothreitol (DTT), 2% (v/v) pharmalyte
398 (pH 3-10) (GE healthcare Japan, Tokyo, Japan), and 1.2 mg ml^{-1} complete protease

399 inhibitor cocktail. The precipitated insoluble proteins were suspended in 5 M urea, 2 M
400 thiourea, 2% (w/v) 3-[(3-cholamidopropyl) dimethylammonio] propanesulfonate
401 (CHAPS), 0.2% (w/v) SDS, 65 mM DTT, 2% (v/v) pharmalyte (pH 3-10), and 1.2 mg
402 ml^{-1} complete protein inhibitor cocktail.
403
404 **SDS-PAGE**
405 Protein samples (0.9 μg) from the culture medium were denatured in 1/6 volume of
406 sample buffer containing 0.125 M Tris-HCl (pH 6.8), 4% (w/v) SDS, 20% (v/v) glycerol,
407 10% (v/v) 2-mercaptoethanol, and 0.004% bromphenol blue at 65°C for 15 min. The
408 samples were resolved using 5–20% (w/v) gradient SDS-PAGE. The proteins in the gels
409 were stained and visualized using Flamingo™ fluorescent gel stain (Bio-Rad
410 Laboratories) or Quick CBB (Wako, Osaka, Japan), according to the manufacturers'
411 protocols.
412
413 **2D-gel analysis**
414 Each protein sample (50 μg) was applied to isoelectrofocusing (IEF) gel strips with an
415 immobilized linear pH gradient (Immobiline™ DryStrip pH 3–10 NL, 18 cm, GE
416 Healthcare, Japan). The strips were rehydrated at 20°C for 12 h at 100 V in solutions
417 containing 6 M urea, 2 M thiourea, 2% (v/v) Triton X-100, 13 mM DTT, 1% (v/v)
418 pharmalyte (pH 3-10), 2.5 mM acetate, and 0.025‰ (w/v) Orange G. The samples were
419 applied to IEF at 20°C on a Cool phoreStar IPG-IEF Type-P system (Anatech,
420 Poughkeepsie, NY) with a stepwise increase in voltage (500 V [2 h], 700 V [1 h], 1,000 V
421 [1 h], 1,500 V [1 h], 2,000 V [1 h], 2,500 V [1 h], 3,000 V [1 h], and 3,500 V [10 h]). The
422 gel strips were equilibrated in a denaturing solution containing 6 M urea, 13 mM DTT,

30% (w/v) glycerol, 2% (w/v) SDS, and 25 mM Tris-HCl (pH 6.8). Denatured gel strips were equilibrated in a reducing and alkylating solution containing 25 mM Tris-HCl (pH 6.8), 2% (w/v) SDS, 0.025‰ (w/v) bromophenol blue, 30% (w/v) glycerol, and 0.24 M iodoacetamide. Next, the gel strips were subjected to 12.5% SDS-PAGE. The protein spots on the gels were stained and visualized using Flamingo™ fluorescent gel stain, according to the manufacturer's instructions.

Peptide preparation for LC-MS/MS analysis

We separated the proteins recovered from each medium using SDS-PAGE. Aliquots (0.9 μg) of each protein sample were loaded in duplicate and the two lanes for each sample were treated at the same time. The gel sections containing protein bands were sliced into four pieces per sample. Flamingo-stained gels were washed twice with 30% (v/v) HPLC-grade acetonitrile (Kanto Chemical, Tokyo, Japan), washed with 100% acetonitrile and dried under vacuum. The dried gel pieces were treated with 2 μl 0.5 μg μl^{-1} trypsin (sequence grade; Promega, Madison, WI) in 50 mM ammonium bicarbonate (Shevchenko and Shevchenko 2001) and incubated at 37°C for 16 h. The digested peptides in the gel pieces were recovered twice with 20 μl 5% (v/v) formic acid/50% (v/v) acetonitrile. Finally, combined extracts were concentrated under vacuum.

Mass spectrometric analysis and database search

LC-MS/MS analyses were performed using an LTQ-Orbitrap XL-HTC-PAL-Paradigm MS4 system (Thermo Fisher Scientific, Bremen, Germany). Trypsin-digested peptides were loaded on the column (100 μm i.d. × 15 cm; L-Column, CERI, Auburn, CA) using a Paradigm MS4 HPLC pump (Michrom BioResources) and HTC-PAL autosampler (CTC

analytics, Zwingen, Switzerland). The digests were applied to a column equilibrated with 6.4% acetonitrile and 0.1% acetic acid. The proteins were eluted under a linear gradient from 6.4 to 41.6% acetonitrile solution containing 0.1% acetic acid over 25 min. The eluted peptides were applied directly to the LTQ-Orbitrap mass spectrometer at a flow rate of 300 nl min^{-1} and a spray voltage of 2.0 kV. The range of MS scan was *m/z* 200–2,000 and the top three peaks were subjected to MS/MS analysis. The obtained spectra were compared against a genome database of *Chlamydomonas reinhardtii* v3.0 from the Joint Genome Institute (http://genome.jgi-psf.org/Chlre3/Chlre3.home.html) using the MASCOT server (version 2.1 Matrix Science, London, UK). The MASCOT search parameters were as follows: threshold at 0.05 in the ion score cut-off, peptide tolerance at 10 ppm, MS/MS tolerance at ± 0.8 Da, peptide charge of 2 + or 3 +, trypsin as the enzyme allowing up to one missed cleavage, carbamidomethylation on cysteine as a fixed modification, and oxidation on methionine as a variable modification. To predict the subcellular localization of identified proteins, we used SignalP, ChloroP, and TargetP from the CBS prediction servers (http://www.cbs.dtu.dk/services/).

Observation of mating of gamates

C. reinhardtii strains mt^+ and mt^- were mixed and then microscope image was taken 10 minutes later. The mating efficiency was determined as described by Chiang et al. (1970).

Acknowledgments

This work was supported by a Grant in-Aid for Scientific Research for a Plant Graduate Student from the Nara Institute of Science and Technology (NAIST), Japan (M.B.). We are grateful to Drs. Y. Fukao and M. Fujiwara of NAIST for their assistance with

proteome analysis, to Dr. T. Sasaki of Okayama University, Japan, for his consultation on the preparation of extracellular and cellular proteins, and to Dr. Y. Hanawa of the National Institute of Advanced Industrial Science and Technology, International Patent Organism Depositary of Japan for his helpful suggestions.

References

Abe, J., Kubo, T., Takagi, Y., Saito, T., Miura, K., Fukuzawa, H., et al. (2004) The transcriptional program of synchronous gametogenesis in *Chlamydomonas reinhardtii*. *Curr. Genet.* 46: 304–315.

Adair, W.S. (1985) Characterization of *Chlamydomonas* sexual agglutinins. *J. Cell Sci.* 2 (Suppl): 233–260.

Aizawa, K. and Miyachi, S. (1986) Carbonic anhydrase and CO_2 concentrating mechanisms in microalgae and cyanobacteria. *FEMS Microbiol. Rev.* 39: 215–233.

Allen, M.D., del Campo, J.A., Kropat, J. and Merchant, S.S. (2007) *FEA1, FEA2*, and *FRE1*, encoding two homologous secreted proteins and a candidate ferrireductase, are expressed coordinately with *FOX1* and *FTR1* in iron-deficient *Chlamydomonas* reinhardtii. *Eukaryot. Cell* 6: 1841–1852.

Baba, M., Hanawa, Y., Suzuki, I. and Shiraiwa, Y. (2011) Regulation of the expression of *H43/Fea1* by multi-signals. *Photosynth. Res.* DOI 10.1007/s11120-010-9619-8.

Badger, M.R. (1987) The CO_2 concentrating mechanism in aquatic phototrophs. In *The Biochemistry of Plants: A Comprehensive Treatise*, *Photosynthesis*, Vol. 10. Edited by Hatch, M.D. and Boardman, N.K. pp. 219–274. Academic Press, NY.

Badger, M.R., Kaplan, A. and Berry, J.A. (1980) Internal inorganic carbon pool of *Chlamydomonas reinhardtii*. Evidence for a CO_2 concentrating mechanism. *Plant*

Physiol. 66: 407–413.

Badger, M.R. and Price, G.D. (2003) CO_2 concentrating mechanisms in cyanobacteria: molecular components, their diversity and evolution. *J. Exp. Bot.* 54: 609–622.

Badger, M.R., Price, G.D., Long, B.M. and Woodger, F.J. (2006) The environmental plasticity and ecological genomics of the cyanobacterial CO_2 concentrating mechanism. *J. Exp. Bot.* 57: 249–265.

Beck, C.F. and Acker, A. (1992) Gametic differentiation of *Chlamydomonas reinhardtii* control by nitrogen and light. *Plant Physiol.* 98: 822–826.

Buchanan, M.J. and Snell, W.J. (1988) Biochemical studies on lysin, a cell wall degrading enzyme released during fertilization in *Chlamydomonas*. *Exp. Cell Res.* 179: 181–193.

Buyanovsky, G.A. and Wagner, G.H. (1983) Annual cycles of carbon dioxide level in soil air. *Soil Sci. Soc. Am. J.* 47: 1139–1145.

Chiang, K.-S., Kates, J.R., Jones, R.F., and Sueoka, N. (1970) On the formation of a homogeneous zygotic population in *Chlamydomonas reinhardtii*. *Dev. Biol.* 22: 655-669.

Coleman, J.R. and Grossman, A.R. (1984) Biosynthesis of carbonic anhydrase in *Chlamydomonas reinhardtii* during adaptation to low CO_2. *Proc. Natl. Acad. Sci. U.S.A.* 81: 6049–6053.

Duanmu, D., Miller, A., Horken, K., Weeks, D. and Spalding, M. (2009) Knockdown of limiting-CO_2-induced gene HLA3 decreases HCO_3-transport and photosynthetic Ci affinity in *Chlamydomonas reinhardtii*. *Proc. Natl. Acad. Sci. U.S.A.* 106: 5990–5995.

Ertl, H., Hallmann, A., Wenzl, S. and Sumper, M. (1992) A novel extensin that may organize extracellular matrix biogenesis in *Volvox carteri*. *EMBO J.* 11: 2055–2062.

Falkowski, P.G. and Raven, J.A. (2007) *Aquatic photosynthesis*, 2nd Ed. pp. 156–200.

519 Princeton University Press, Princeton, NJ.
520 Fei, X., Eriksson, M., Yang, J. and Deng, X. (2009) An Fe deficiency responsive element
521 with a core sequence of TGGCA regulates the expression of *Fea1* in *Chlamydomonas*
522 *reinharditii*. *J. Biochem* 146: 157–166.
523 Fujiwara, S., Ishida, N., and Tsuzuki, M. (1996) Circadian expression of the carbonic
524 anhydrase gene, *Cah1*, in *Chlamydomonas reinhardtii*. *Plant Mol. Biol.* 32: 745–749.
525 Fukuzawa, H., Fujiwara, S., Yamamoto, Y., Dionisio-Sese, M.L., and Miyachi, S. (1990)
526 cDNA cloning, sequence, and expression of carbonic anhydrase in *Chlamydomonas*
527 *reinhardtii*: Regulation by environmental CO_2 concentration. *Proc. Natl Acad. Sci.*
528 *U.S.A.* 87: 4383–4387.
529 Goodenough, U.W., Gebhart, B., Mecham, R.E. and Heuser, J.E. (1986) Crystals of the
530 *Chlamydomonas reinhardtii* cell wall: Polymerization, depolymerization, and
531 purification of glycoprotein monomers. *J. Cell Biol.* 103: 405–417.
532 Hallmann, A. (2006) The pherophorins: Common, versatile building blocks in the
533 evolution of extracellular matrix architecture in Volvocales. *Plant J*. 45: 292–307.
534 Hanawa, Y., Iwamoto, K. and Shiraiwa, Y. (2004) Purification of a recombinant H43, a
535 high-CO_2-inducible protein of *Chlamydomonas reinhardtii*, expressed in *Escherichia*
536 *coli*. *Jpn. J. Phycol. (Sôrui)* 52 (Suppl): 95–100.
537 Hanawa, Y., Watanabe, M., Karatsu, Y., Fukuzawa, H. and Shiraiwa, Y. (2007) Induction
538 of a high-CO_2-inducible, periplasmic protein, H43, and its application as a
539 high-CO_2-responsive marker for study of the high-CO_2-sensing mechanism in
540 *Chlamydomonas reinhardtii*. *Plant Cell Physiol.* 48: 299–309.
541 Harris, E.H. (2009) *The Chlamydomonas Sourcebook*, 2nd Ed, Vol. 1. p. 120. Academic
542 Press, San Diego, CA.

543 Hoffmann, X.K. and Beck C.F. (2005) Mating-induced shedding of cell walls, removal of
544 walls from vegetative cells, and osmotic stress induce presumed cell wall genes in
545 *Chlamydomonas*. *Plant Physiol.* 139: 999–1014.
546 Ishihama, Y., Oda, Y., Tabata, T., Sato, T., Nagasu, T., Rappsilber, J., et al. (2005)
547 Exponentially modified protein abundance index (emPAI) for estimation of absolute
548 protein amount in proteomics by the number of sequenced peptides per protein. *Mol.*
549 *Cell. Proteomics* 4: 1265–1272.
550 Iwasaki, I., Hu, Q., Kurano, N. and Miyachi, S. (1998) Effect of extremely high-CO_2
551 stress on energy distribution between photosystem I and photosystem II in a
552 'high-CO_2' tolerant green alga, *Chlorococcum littorale* and the intolerant green alga
553 *Stichococcus bacillaris*. *J. Photochem. Photobiol. B: Biol.* 44: 184–190.
554 Jia, Y., Xue, L., Liu, H. and Li, J. (2009) Characterization of the
555 glyceraldehyde-3-phosphate dehydrogenase (GAPDH) gene from the halotolerant
556 alga *Dunaliella salina* and inhibition of its expression by RNAi. *Curr. Microbiol.* 58:
557 426–431.
558 Kaplan, A. and Reinhold, L. (1999) CO_2 concentrating mechanisms in photosynthetic
559 microorganisms. *Annu. Rev. Plant Physiol. Plant Mol. Biol.* 50: 539–570.
560 Kimpel, D.L., Togasaki, R.K. and Miyachi, S. (1983) Carbonic anhydrase in
561 *Chlamydomonas reinhardtii* I. Localization. *Plant Cell Physiol.* 24: 255–259.
562 Kinoshita, T., Fukuzawa, H., Shimada, T., Saito, T. and Matsuda, Y. (1992) Primary
563 structure and expression of a gamete lytic enzyme in *Chlamydomonas reinhardtii*:
564 similarity of functional domains to matrix metalloproteases. *Proc. Natl Acad. Sci.*
565 *U.S.A.* 89: 4693–4697.
566 Kobayashi, H., Odani, S. and Shiraiwa, Y. (1997) A high-CO_2-inducible, periplasmic

567 polypeptide in an unicellular green alga *Chlamydomonas reinhardtii* (abstract no. 493).
568 *Plant Physiol.* 114: S112.
569 Kubo, T., Saito, T., Fukuzawa, H. and Matsuda, Y. (2001) Two tandemly-located matrix
570 metalloprotease genes with different expression patterns in the *Chlamydomonas*
571 sexual cell cycle. *Curr. Genet.* 40: 136–143.
572 Lee, J.-H., Waffenschmidt, S., Small, L. and Goodenough, U. (2007) Between-species
573 analysis of short-repeat modules in cell wall and sex-related hydroxyproline-rich
574 glycoproteins of *Chlamydomonas. Plant Physiol.* 144: 1813–1826.
575 Mariscal, V., Moulin, P., Orsel, M., Miller, A.J., Emilio Fernández, E. and Galvána, A.
576 (2006) Differential regulation of the *Chlamydomonas Nar1* gene family by carbon and
577 nitrogen. *Protist* 157 :421–433.
578 Miura, K., Yamano, T., Yoshioka, S., Kohinata, T., Inoue, Y., Taniguchi, F., et al. (2004)
579 Expression profiling-based identification of CO_2-responsive genes regulated by
580 CCM1 controlling a carbon concentrating mechanism in *Chlamydomonas reinhardtii*.
581 *Plant Physiol*. 135: 1595–1607.
582 Miyachi, S., Iwasaki, I. and Shiraiwa, Y. (2003) Historical perspective on microalgal and
583 cyanobacterial acclimation to low and extremely high CO_2 conditions. *Photosynth.*
584 *Res.* 77: 139–153.
585 Moroney, J.V. and Ynalvez, R.A. (2007) A proposed carbon dioxide concentration
586 mechanism in *Chlamydomonas reinhardtii*. *Eukaryot. Cell* 6: 1251–1259.
587 Pazour, G.J., Agrin, N., Leszyk, J. and Witman, G.B. (2005) Proteomic analysis of a
588 eukaryotic cilium. *J. Cell Biol*. 170: 103–113.
589 Raven, J.A., Cockell, C.S. and De La Rocha, C.L. (2008) The evolution of inorganic
590 carbon concentrating mechanisms in photosynthesis. *Philos. Trans. R. Soc. Lond., B,*

591 *Biol. Sci.* 363: 2641–2650.
592 Reichi, P.B., Hungate, B.A. and Luo, Y. (2006) Carbon-nitrogen interactions in terrestrial
593 ecosystems in response to rising atmospheric carbon dioxide. *Annu. Rev. Ecol. Evol.*
594 *Syst.* 37: 611–636.
595 Rexach, J., Fernández, E. and Galván, A. (2000) The *Chlamydomonas reinhardtii* Nar1
596 gene encodes a chloroplast membrane protein involved in nitrite transport. *Plant Cell*
597 12: 1441–1453.
598 Rubinelli, P., Siripornadulsil, S., Gao-Rubinelli, F. and Sayre, R.T. (2002) Cadmium- and
599 iron-stress-inducible gene expression in the green alga *Chlamydomonas reinhardtii*:
600 Evidence for H43 protein function in iron assimilation. *Planta* 215: 1–13.
601 Sager, R. and Granick, S. (1954) Nutritional control of sexuality in *Chlamydomonas*
602 *reinhardtii*. *J. Gen. Physiol.* 5: 729–742.
603 Sasaki, T., Kurano, N. and Miyachi, S. (1998) Induction of ferric reductase activity and of
604 iron uptake capacity in *Chlorococcum littorale* cells under extremely high-CO_2 and
605 iron-deficient conditions. *Plant Cell Physiol.* 39: 405–410.
606 Satoh, A., Kurano, N. and Miyachi, S. (2001) Inhibition of photosynthesis by intracellular
607 carbonic anhydrase in microalgae under excess concentrations of CO_2. *Photosynth.*
608 *Res.* 68: 215–224.
609 Satoh, A., Kurano, N., Harayama, S. and Miyachi, S. (2004) Effects of chloramphenicol
610 on photosynthesis, protein profiles and transketolase activity under extremely high
611 CO_2 concentration in an extremely-high-CO_2-tolerant green microalga, *Chlorococcum*
612 *littorale*. *Plant Cell Physiol*. 45: 1857–1862.
613 Satoh, A., Kurano, N., Senger, H. and Miyachi, S. (2002) Regulation of energy balance in
614 photosystems in response to changes in CO_2 concentrations and light intensities during

615 growth in extremely-high-CO_2-tolerant green microalgae. *Plant Cell Physiol.* 43:
616 440–451.
617 Sears, B.B., Boynton, J.E. and Gillham, N.W. (1980) The effect of gametogenesis
618 regimes on the chloroplast genetic system of *Chlamydomonas reinhardtii. Genetics.*
619 96: 95–114
620 Shiraiwa, Y. and Miyachi, S. (1985) Effects of temperature and CO_2 concentration on
621 induction of carbonic anhydrase and changes in efficiency of photosynthesis in
622 *Chlorella vulgaris* 11h. *Plant Cell Physiol.* 26: 543–549.
623 Soupene, E., Inwood, W. and Kustu, S. (2004) Lack of the Rhesus protein Rh1 impairs
624 growth of the green alga *Chlamydomonas reinhardtii* at high CO_2. *Proc. Natl Acad. Sci.*
625 *U.S.A.* 101: 7787–7792.
626 Spalding, M.H. (2008) Microalgal carbon-dioxide-concentrating mechanisms:
627 *Chlamydomonas* inorganic carbon transporters. *J. Exp. Bot.* 59: 1463–1473.
628 Stolzy, L.H. (1974) Soil atmosphere. In *The Plant Root and Its Environment.* Edited by
629 EW Carson. pp 335–362. University Press of Virginia, Charlottesville, VA.
630 Sueoka, N. (1960) Mitotic replication of deoxyribonucleic acid in *Chlamydomonas*
631 *reinhardi*. *Proc. Natl Acad. Sci. U.S.A.* 46: 83–91.
632 Wienkoop, S., Weiss, J., May, P., Kempa, S., Irgang, S., Recuenco-Munoz, L., et al.
633 (2010) Targeted proteomics for *Chlamydomonas reinhardtii* combined with rapid
634 subcellular protein fractionation, metabolomics and metabolic flux analyses. *Mol.*
635 *Biosyst.* 6: 1018–1031.
636 Yamano, T. and Fukuzawa, H. (2009) Carbon-concentrating mechanism in a green alga,
637 *Chlamydomonas reinhardtii*, revealed by transcriptome analyses. *J. Basic Microbiol.*
638 49: 42–51.

639 Yang, S.Y., Tsuzuki, M. and Miyachi, S. (1985) Carbonic anhydrase of *Chlamydomonas*:
640 Purification and studies on its induction using antiserum against *Chlamydomonas*
641 carbonic anhydrase. *Plant Cell Physiol*. 26: 25–34.
642 Zheng, Z.L. (2009) Carbon and nitrogen nutrient balance signaling in plants. *Plant Signal.*
643 *Behav.* 4(7): 584–591.
644

645 **Figure legends**

646

647 **Fig. 1.** Growth parameters of the wall-less strain *Chlamydomonas reinhardtii* CC-400
648 under various CO_2 conditions in a batch culture. **A**, Growth curves. Air (●), cells
649 pre-grown in ordinary air for 3 days were transferred to fresh medium under the same
650 conditions; Air to CO_2 (■), cells pre-grown in ordinary air for 3 days were transferred to
651 fresh medium under high-CO_2 conditions (3% CO_2 in air); CO_2 (▲), cells pre-grown in
652 air containing 3% CO_2 for 3 days were transferred to fresh medium under the same
653 conditions. **B**, Specific growth rate (*y*-axis) and the doubling time (numbers on the
654 columns) during the logarithmic growth phase under various CO_2 conditions. Values
655 were calculated from those in Fig. 1A.

656

657 **Fig. 2.** Semi-continuous culture of the wall-less strain *Chlamydomonas reinhardtii*
658 CC-400 for the preparation of samples for proteomic analysis. A, Experimental plan of
659 semi-continuous culture with dilution of culture once per day to maintain logarithmic
660 growth. Algal cells were grown in ordinary air for 3 days and then transferred to 3%
661 CO_2-enriched air. Cells were harvested 0 (1), 1 (2), and 3 (3) days after the transfer of
662 cells from air to high-CO_2. Three independent replicates were used. B, Specific growth
663 rates and the doubling time of cells in cultures (1), (2), and (3) were 9.19 ± 0.32,
664 6.19 ± 0.55, and 5.98 ± 0.09 h, respectively. C, Concentrations of total proteins released
665 into the medium in cultures (1)–(3) shown in Fig. 2A. D, SDS-PAGE image stained with
666 Flamingo™ gel stain. CAH1 and H43/FEA1 are markers of air- and high-CO_2-inducible
667 proteins in *C. reinhardtii*, respectively. Lanes 1–3 show triplicate samples.

668

669 **Fig. 3.** A Venn diagram of extracellular proteins identified in air-, 1-day-high-CO_2-, and
670 3-day-high-CO_2-acclimated cells. Numbers in parenthesis indicate numbers of secretory
671 proteins which were identified in air-, 1-day-high-CO_2-, and/or
672 3-day-high-CO_2-acclimated cells, respectively. Percentages indicate contents of secretory
673 protein in total.
674
675 **Fig. 4.** Lists of top 10 extracellular proteins aligned by its protein content and by its ratio
676 of protein content in air- to 1-day-high-CO_2- or 3-day-high-CO_2-acclimated cells.
677
678 **Fig. 5.** Microscopic images of mating. **A**, the mixture of *C. reinhardtii* CC-620 and
679 CC-621 which had been grown under high-CO_2 conditions. **B**, higher magnification
680 image of A. **C**, the mixture of *C. reinhardtii* CC-620 and CC-621 which had been grown
681 under nitrogen-free conditions. **D**, higher magnification image of C.
682
683 (Additional information)
684 The English in this document has been checked by at least two professional editors, both native
685 speakers of English. For a certificate, please see:
686 http://www.textcheck.com/certificate/ZtGAp9
687

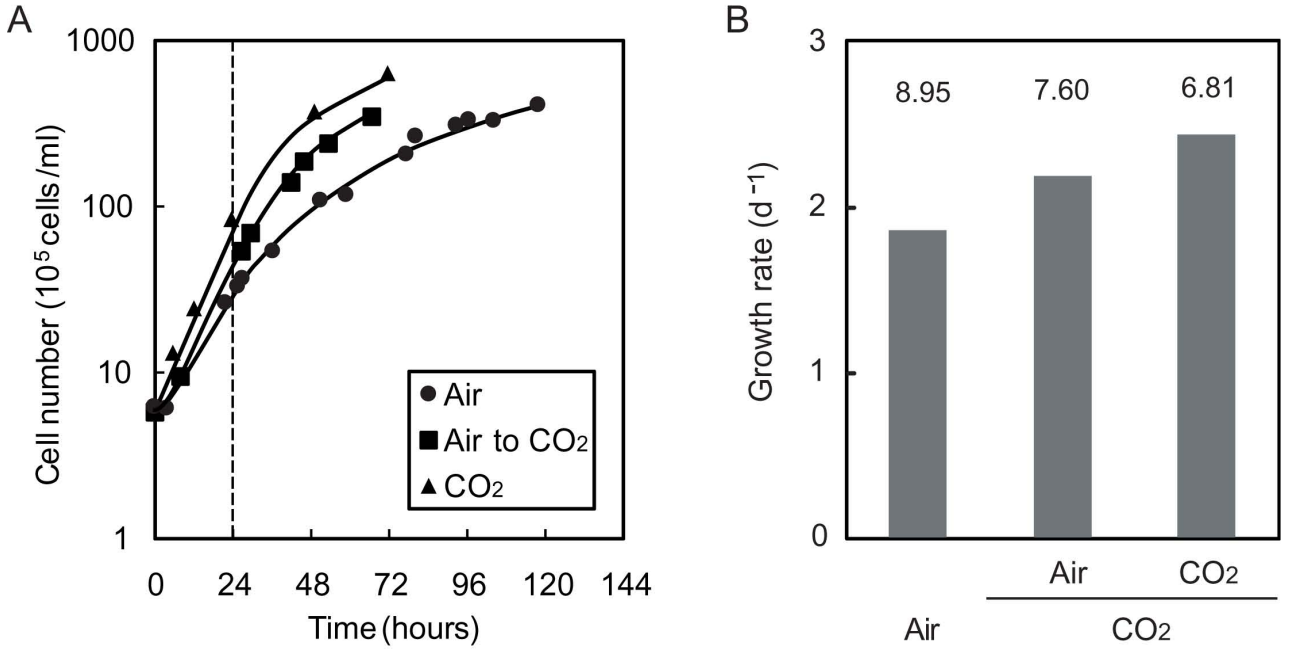
A
1000
100
10
1
Cell number (10^5 cells/ml)
0
24
48
72
96
120
144
Time (hours)
Air
Air to CO_2
CO_2
B
3
2
1
0
Growth rate (d^{-1})
8.95
7.60
6.81
Air
Air
CO_2
CO_2

Fig.1

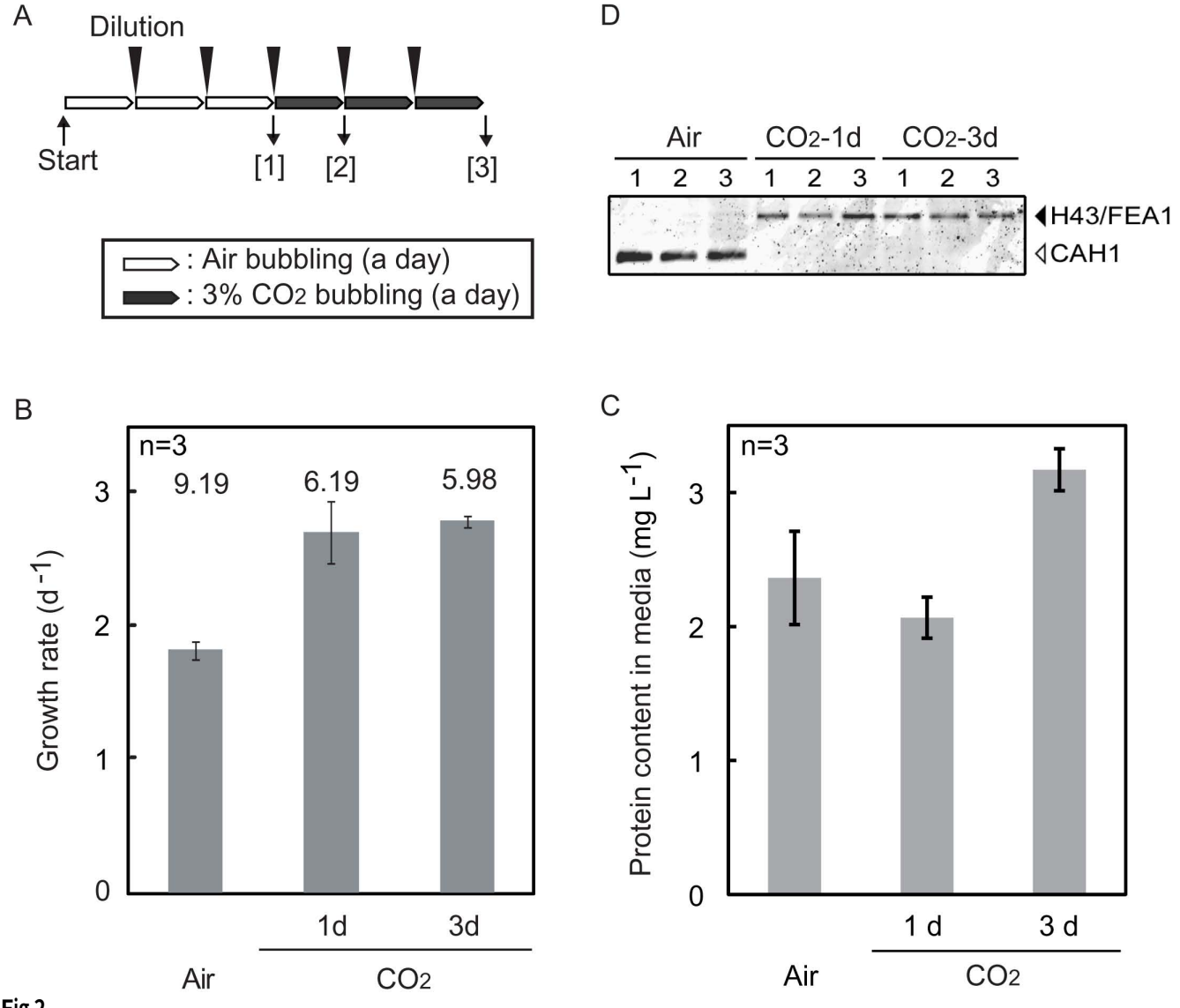
A
Dilution
Start
[1]
[2]
[3]
: Air bubbling (a day)
: 3% CO2 bubbling (a day)
D
Air
CO2-1d
CO2-3d
1 2 3 1 2 3 1 2 3
H43/FEA1
CAH1
B
n=3
9.19
6.19
5.98
Growth rate (d -1)
0
1
2
3
Air
1d
3d
CO2
C
n=3
Protein content in media (mg L-1)
0
1
2
3
Air
1 d
3 d
CO2

Fig.2

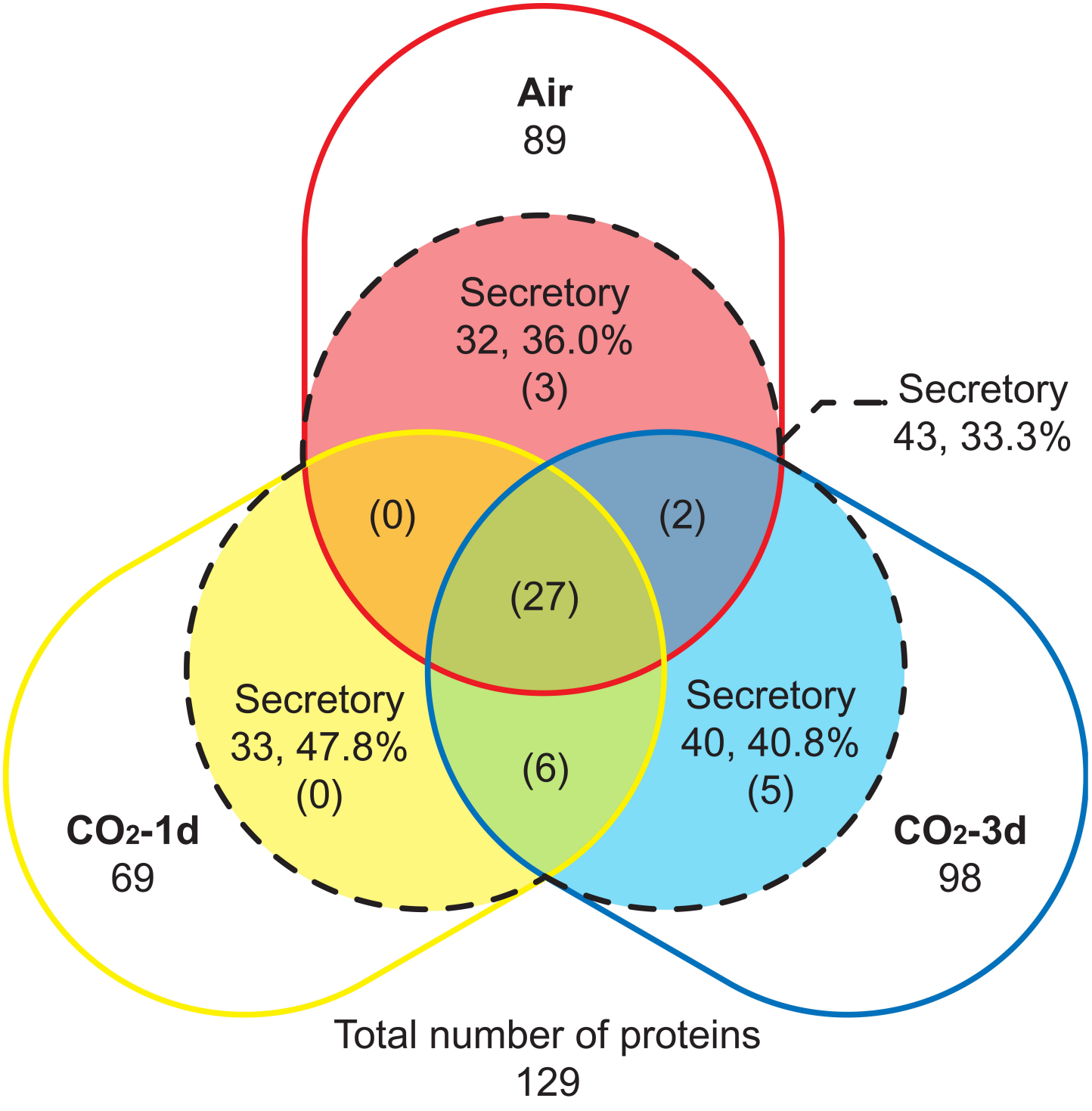
Air
89
Secretory
32, 36.0%
(3)
Secretory
43, 33.3%
(0)
(2)
(27)
Secretory
33, 47.8%
(0)
Secretory
40, 40.8%
(5)
(6)
CO2-1d
69
CO2-3d
98
Total number of proteins
129

Fig.3

Air		Air/CO_2-3d	
Protein	Amount	Protein	Ratio
CAH1	10.11	CAH1	5.85
H43/FEA1	6.04	GAP3	5.25
EXC1	5.37	CAH1 /CAH2	2.29
GAP3	4.95	PHC4	1.90
PHC21	3.96	PHOT	1.67
EXC2	3.49	GP1	1.49
GP1	2.09	EXC1	1.43
FAP211	1.90	PCY1	1.41
GP2	1.79	FAP211	1.26
HCI2	1.75	RPS14	1.14

CO_2-1d		CO_2-1d/Air	
Protein	Amount	Protein	Ratio
H43/FEA1	22.09	H43/FEA1	3.66
EXC2	4.92	ISG-C1	3.57
PHC21	4.82	HCI3	3.45
EXC1	4.77	FAP102	2.26
HCI3	3.43	HCI1	2.07
HCI2	3.36	HCI2	1.93
FAP102	3.16	FAP212	1.74
GP1	3.06	GP2	1.60
GP2	2.87	GP1	1.46
FAP211	2.32	EXC2	1.41

CO_2-3d		CO_2-3d/Air	
Protein	Amount	Protein	Ratio
H43/FEA1	26.01	ISG-C1	4.36
EXC1	3.76	H43/FEA1	4.31
FAP102	3.48	HCI3	3.03
HCI3	3.02	FAP102	2.48
ISG-C1	2.46	FAP212	1.85
HCI2	2.46	GAS31	1.80
GP2	2.36	HCI1	1.41
ISG-C2	2.27	HCI2	1.41
GAS31	1.93	GP2	1.32
CAH1	1.73	SRR16	1.12

Fig.4

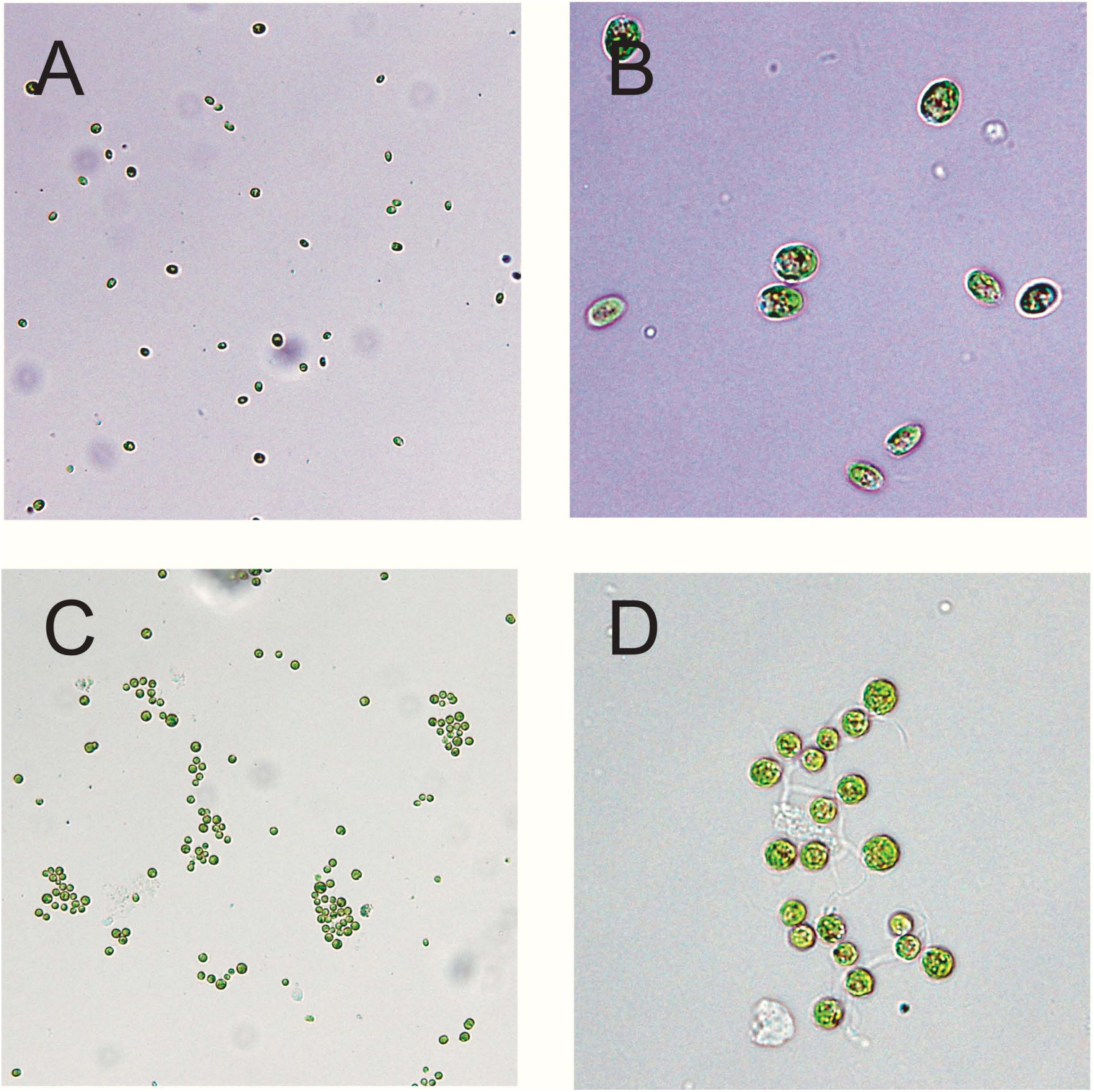

Fig.5

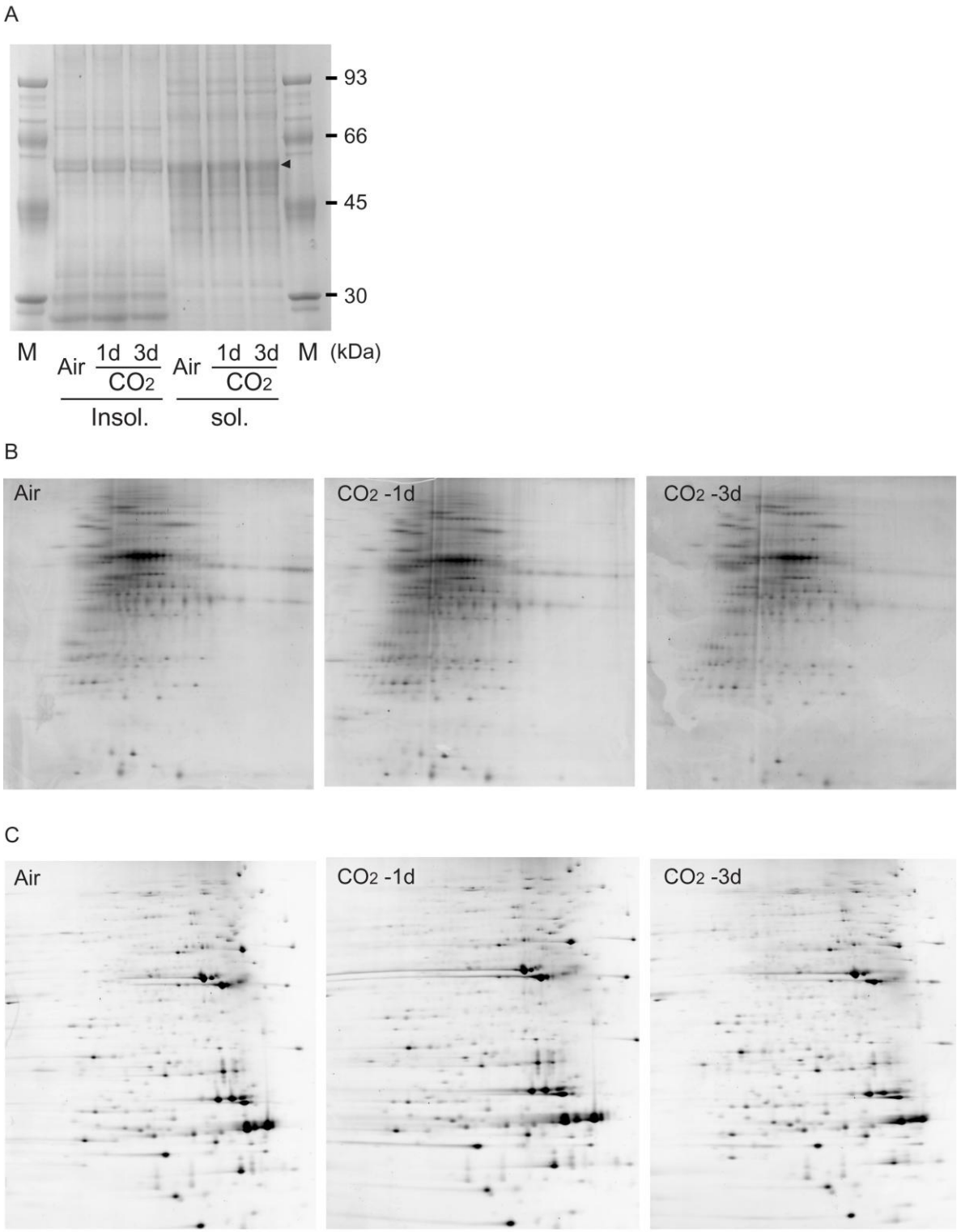

Fig. S1. 2D-GE analysis of proteins in the intracellular-soluble and -insoluble fractions from a wall-less strain of *Chlamydomonas reinhardtii* CC-400 grown under various CO_2 conditions. A, SDS-PAGE of the cellular-soluble and -insoluble proteins stained with Quick-CBB. M indicates a molecular weight marker. The arrowhead indicates a band corresponding to the large subunit of Rubisco. B and C, 2D-GE profiles of the cellular-soluble and -insoluble proteins stained with Flamingo™ gel stain. Air, CO_2-1d and CO_2-3d represent samples (1), (2), and (3) from Fig. 2A, respectively.

Table 1 List of top 20 extracellular proteins aligned by its amount in air-acclimated cells.

Ranking	Assigned name	JGI protein ID	Protein content in Air (mol%)	Air/CO_2-3d	SignalP	Function and/or similarities to known proteins	Grouping
1	CAH1	24120 *	10.11 ± 2.84	5.85	S	Carbonic anhydrase1(CAH1), low-CO2 inducible gene regulated by LCR1 [PMID: 15155888] and CCM1 [PMID: 11287669]	CAH
2	H43/FEA1	129929	6.04 ± 5.50	0.23	S	high-CO2 inducible, iron-deficiency inducible, periplasmic protein [PMID: 17660359]; Also known as H43[PMID: 17202179]	other
3	EXC1	191447	5.37 ± 2.59	1.43	S	No domain	-
4	GAP3	129019 *	4.95 ± 3.22	5.25	C	Glyceraldehyde 3-phosphate dehydrogenase A	other
5	PHC21	93464	3.96 ± 2.25	-	C	pherophorin-C21 (PHC21) [PMID: 16367971]; similar to	PHC
6	EXC2	152521	3.49 ± 2.04	-	C	No domain	-
7	GP1	34358	2.09 ± 0.29	1.49	S	GP1[CAL91937], hydroxyproline-rich glycoprotein [PMID:	GP
8	FAP211	186474	1.90 ± 0.95	1.26	S	FAP211 [PMID: 15998802], similar to NSG1[PMID: 15459796]	NSG
9	GP2	195768	1.79 ± 0.63	0.76	S	GP2[CAL91937], hydroxyproline-rich glycoprotein [PMID:	GP
10	HCI2	190800	1.75 ± 0.76	0.71	_	similar to flagella associated protein; NSG1protein [PMID:	NSG
11	PCY1	185915	1.68 ± 1.23	1.41	M	pre-apoplastocyanin, PETE [PMID: 2165059;PMID: 8940133]	other
12	FAP102	191022	1.40 ± 1.14	0.40	S	FAP102 [PMID: 15998802], similar to GP3 [CAJ98661]	GP
13	LCI5	196466	1.37 ± 0.91	-	C	low-CO2-inducible protein, regulated by CCM1 [PMID: 15235119]	other
14	CAH1/CAH2	24120; 128726 *	1.37 ± 0.18	2.29	S	Carbonic anhydrase1(CAH1); Carbonic anhydrase 2 (CAH2), high-CO2-inducible [PMID: 2124702]	CAH
15	FSD1	182933	1.32 ± 0.30	-	C	superoxide dismutase [Fe]	other
16	SEBP1	189186	1.15 ± 0.76	-	C	Sedoheptulose-1,7-bisphosphatase	other
17	GAS31	193780	1.07 ± 0.92	0.56	S	GAS31[PMID: 16183845], belongs to the large pherophorin-family	GAS
18	HCI3	186476	1.00 ± 0.37	0.33	_	similar to flagella associated protein; NSG1protein [PMID:	NSG
19	HCI1	115272	0.96 ± 0.09	0.71	S	similar to NSG1(nitrogen-starved gametogenesis) protein [PMID: 15459796]	NSG
20	FAP212	186478	0.90 ± 0.02	0.54	S	FAP212 [PMID: 15998802], similar to NSG1[PMID: 15459796]	NSG

*: Protein content was significantly($p<0.05$) higher than that of CO2-3d

Table 2 List of top 20 extracellular proteins aligned by its amount in 1-day-high-CO_2-acclimated cells.

Ranking	Assigned name	JGI protein ID	Protein content in CO_2-1d (mol%)	CO_2-1d/Air	SignalP	Function and/or similarities to known proteins	Grouping
1	H43/FEA1	129929 *	22.09 ± 8.16	3.66	S	high-CO2 inducible, iron-deficiency inducible, periplasmic protein [PMID: 17660359]; Also known as H43[PMID: 17202179]	other
2	EXC2	152521	4.92 ± 0.62	1.41	C	No domain	-
3	PHC21	93464	4.82 ± 0.97	1.22	C	pherophorin-C21 (PHC21) [PMID: 16367971]; similar to	PHC
4	EXC1	191447	4.77 ± 1.39	0.89	S	No domain	-
5	HCI3	186476	3.43 ± 3.09	3.45	_	similar to flagella associated protein; NSG1protein [PMID:	NSG
6	HCI2	190800 *	3.36 ± 0.79	1.93	_	similar to flagella associated protein; NSG1protein [PMID:	NSG
7	FAP102	191022 *	3.16 ± 0.40	2.26	S	FAP102 [PMID: 15998802], similar to GP3 [CAJ98661]	GP
8	GP1	34358 *	3.06 ± 0.30	1.46	S	GP1[CAL91937], hydroxyproline-rich glycoprotein [PMID:	GP
9	GP2	195768	2.87 ± 0.79	1.60	S	GP2[CAL91937], hydroxyproline-rich glycoprotein [PMID:	GP
10	FAP211	186474	2.32 ± 1.35	1.22	S	FAP211 [PMID: 15998802], similar to NSG1[PMID: 15459796]	NSG
11	ISG-C1	178049 *	2.02 ± 0.44	3.57	S	similar to Volvox ISG [PMID: 1600938] and Chlamydomonas VSP-3 [PMID: 8000007]; Also known as FAP40 [PMID:	ISG
12	HCI1	115272 *	1.99 ± 0.68	2.07	S	similar to NSG1(nitrogen-starved gametogenesis) protein [PMID: 15459796]	NSG
13	FAP212	186478	1.57 ± 0.66	1.74	S	FAP212 [PMID: 15998802], similar to NSG1[PMID: 15459796]	NSG
14	ISG-C4	185383 *	1.51 ± 0.62	-	S	similar to Volvox ISG [PMID: 1600938] and Chlamydomonas VSP-3 [PMID: 8000007]; Also known as FAP137 [PMID:	ISG
15	GAS31	193780	1.41 ± 0.79	1.32	S	GAS31[PMID: 16183845], belongs to the large pherophorin-family	GAS
16	CAH1	24120	1.41 ± 0.17	0.14	S	Carbonic anhydrase1(CAH1), low-CO2 inducible gene regulated by LCR1 [PMID: 15155888] and CCM1 [PMID: 11287669]	CAH
17	GAP3	129019	0.99 ± 1.08	0.20	C	Glyceraldehyde 3-phosphate dehydrogenase A	other
18	PHC1	196399	0.95 ± 0.36	-	S	pherophorin-C1 (PHC1) [PMID: 16367971; belongs to the large pherophorin-family	PHC
19	EXC3	166267	0.82 ± 0.13	1.13	S	Hypothetical protein containing a DUF3707; pherophorin domain	PHC
20	PCY1	185915	0.72 ± 0.35	0.43	M	pre-apoplastocyanin, PETE [PMID: 2165059;PMID: 8940133]	other

*: Protein content was significantly($p<0.05$) higher than that of Air

Table 3 List of top 20 extracellular proteins aligned by its amount in 3-day-high-CO_2-acclimated cells.

Ranking	Assigned name	JGI protein ID	Protein content in CO_2-3d (mol%)	CO_2-3d/Air	SignalP	Function and/or similarities to known proteins	Grouping
1	H43/FEA1	129929 *	26.01 ± 4.30	4.31	S	high-CO2 inducible, iron-deficiency inducible, periplasmic protein [PMID: 17660359]; Also known as H43[PMID: 17202179]	other
2	EXC1	191447	3.76 ± 2.61	0.70	S	No domain	-
3	FAP102	191022 *	3.48 ± 0.63	2.48	S	FAP102 [PMID: 15998802], similar to GP3 [CAJ98661]	GP
4	HCI3	186476 *	3.02 ± 1.52	3.03	_	similar to flagella associated protein; NSG1protein [PMID:	NSG
5	ISG-C1	178049 *	2.46 ± 0.70	4.36	S	similar to Volvox ISG [PMID: 1600938] and Chlamydomonas VSP-3 [PMID: 8000007]; Also known as FAP40 [PMID:	ISG
6	HCI2	190800 *	2.46 ± 0.27	1.41	_	similar to flagella associated protein; NSG1protein [PMID:	NSG
7	GP2	195768	2.36 ± 0.49	1.32	S	GP2[CAL91937], hydroxyproline-rich glycoprotein [PMID:	GP
8	ISG-C2	193727 *	2.27 ± 0.75	-	S	similar to Volvox ISG [PMID: 1600938] and Chlamydomonas VSP-3 [PMID: 8000007]	ISG
9	GAS31	193780	1.93 ± 0.52	1.80	S	GAS31[PMID: 16183845], belongs to the large pherophorin-family	GAS
10	CAH1	24120	1.73 ± 0.24	0.17	S	Carbonic anhydrase1(CAH1), low-CO2 inducible gene regulated by LCR1 [PMID: 15155888] and CCM1 [PMID: 11287669]	CAH
11	FAP103	58944	1.69 ± 1.10	-	_	Flagellar Associated Protein similar to ncleoside diphosphate kinase, found in the flagellar proteome [PMID: 15998802]	other
12	FAP212	186478 *	1.66 ± 0.34	1.85	S	FAP212 [PMID: 15998802], similar to NSG1[PMID: 15459796]	NSG
13	PHC15	148333	1.54 ± 0.87	-	S	pherophorin-C15 (PHC15) [PMID: 16367971]; similar to	PHC
14	FAP211	186474	1.51 ± 0.23	0.79	S	FAP211 [PMID: 15998802], similar to NSG1[PMID: 15459796]	NSG
15	ISG-C4	185383	1.47 ± 0.24	-	S	similar to Volvox ISG [PMID: 1600938] and Chlamydomonas VSP-3 [PMID: 8000007]; Also known as FAP137 [PMID:	ISG
16	GP1	34358	1.40 ± 0.43	0.67	S	GP1[CAL91937], hydroxyproline-rich glycoprotein [PMID:	GP
17	HCI1	115272	1.36 ± 0.73	1.41	S	similar to NSG1(nitrogen-starved gametogenesis) protein [PMID: 15459796]	NSG
18	PCY1	185915	1.19 ± 0.50	0.71	M	pre-apoplastocyanin, PETE [PMID: 2165059;PMID: 8940133]	other
19	HCI4	157979 *	0.96 ± 0.59	-	C	similar to GP3 [CAJ98661]	GP
20	GAP3	129019	0.94 ± 0.16	0.19	C	Glyceraldehyde 3-phosphate dehydrogenase A	other

*: Protein content was significantly($p<0.05$) higher than that of Air

Table S1. List of extracellular proteins in Air-, CO2-1d, and CO2-3d acclimated cells.

Assigned name	Renamed	ProteinID	Air				CO2-1d					CO2-3d					Predicted localization	Function and/or similarities to known proteins
			Protein content (mol%)	Ratio	Highest MASCOT Score	# detected	Protein content (mol%)	Ratio	Highest MASCOT Score	# detected		Protein content (mol%)	Ratio	Highest MASCOT Score	# detected			
HTA9		82	0.885	1	54	1/3	-	-	-	0/3		-	-	-	0/3		_	Histone H2A
RPL27		260	0.763	1	64	1/3	-	-	-	0/3		0.319	0.418	53	1/3		_	Cytosolic 80S ribosomal protein L27; Cytosolic 60S large ribosomal subunit protein L27
MST1		574	-	-	-	0/3	0.066 ± 0.027	-	176	3/3	*	0.124 ± 0.033	-	358	3/3	*	M	Mastigoneme-like protein [PMID: 15998802]
FMG1-2		16132	0.084 ± 0.041	1	265	3/3	-	-	-	0/3		0.017	0.205	62	1/3		S	Flagella membrane glycoprotein 1B [PMID: 8626057]
GPM1B		18029	0.119	1	65	1/3	-	-	-	0/3		-	-	-	0/3		_	Phosphoglucomutase
CAH1		24120	10.109 ± 2.841	1	911	3/3	1.407 ± 0.171	0.139	198	3/3		1.727 ± 0.245	0.171	337	3/3		S	Carbonic anhydrase1(CAH1), low-CO2 inducible gene regulated by LCR1 [PMID: 15155888] and CCM1 [PMID: 11287669]
CGS1		24268	-	-	-	0/3	-	-	-	0/3		0.120	-	64	1/3		C	cystathionine gamma-synthase
RPS14		24344	0.644 ± 0.145	1	68	3/3	0.470 ± 0.045	0.730	68	3/3		0.564 ± 0.359	0.876	68	3/3		_	Cytosolic 80S ribosomal protein S14; Cytosolic 40S small ribosomal subunit protein S14
IDA5		24392	-	-	-	0/3	-	-	-	0/3		0.363 ± 0.128	-	80	3/3	*	_	Actin
TPIC		26265	-	-	-	0/3	-	-	-	0/3		0.153	-	63	1/3		C	triose phosphate isomerase
GP1		34358	2.089 ± 0.294	1	358	3/3	3.055 ± 0.295	1.462	537	3/3	*	1.402 ± 0.431	0.671	422	3/3		S	GP1[CAL91937], hydroxyproline-rich glycoprotein [PMID: 1699225]
PGK1		36313	2.492	1	324	2/3	0.460	0.184	125	2/3		0.374	0.150	136	2/3		C	phosphoglycerate kinase
MSD1		53941	0.318	1	50	1/3	-	-	-	0/3		-	-	-	0/3		_	Superoxide dismutase [Mn]
FAP103		58944	4.712	1	132	2/3	1.598	0.339	106	1/3		1.692 ± 1.101	0.359	178	3/3		_	Flagellar Associated Protein similar to ncleoside diphosphate kinase, found in the flagellar proteome [PMID: 15998802]
RPS15a		59755	-	-	-	0/3	-	-	-	0/3		0.447	-	54	1/3		_	Cytosolic 80S ribosomal protein 15a; Cytosolic 40S small ribosomal subunit protein 15a
MMP1		60542	-	-	-	0/3	0.675 ± 0.752	-	400	3/3	*	0.362 ± 0.104	-	173	3/3	*	_	Matrix Metalloprotease 1(MMP1); known as GLE (Gametic Lytic Enzyme); autolysin; [PMID: 11680823]
RPL15		76376	-	-	-	0/3	-	-	-	0/3		0.275	-	61	1/3		_	Cytosolic 80S ribosomal protein L15; Cytosolic 60S large subunit ribosomal protein L15
ATP1A		76602	0.182	1	73	2/3	-	-	-	0/3		-	-	-	0/3		M	alpha subunit of the mitochondrial ATP synthase
ATP2		78348	0.119	1	50	1/3	-	-	-	0/3		-	-	-	0/3		M	ATP synthase F1F0 beta chain
CRT2		78954	0.244	1	67	1/3	-	-	-	0/3		-	-	-	0/3		Endosome	Calreticulin 2, high-capacity calcium-binding protein [PMID: 17932292]
ESTEXT_GENEWISEW_1.C_520044	EXC18	82208	0.241	1	54	1/3	-	-	-	0/3		-	-	-	0/3		_	Predicted leucyl aminopeptidase
RBCS1		82986	1.311	1	72	1/3	-	-	-	0/3		-	-	-	0/3		C	ribulose bisphosphate carboxylase/oxygenase small subunit 1
PGH1		83064	0.881 ± 0.880	1	316	3/3	0.299	0.340	105	2/3		0.293	0.333	135	2/3		_	Enolase
PHC21		93464	3.963 ± 2.249	1	195	3/3	4.824 ± 0.968	1.217	268	3/3		4.095	1.033	264	2/3		C	pherophorin-C21 (PHC21) [PMID: 16367971]; belongs to the large pherophorin-family
E_GWH.8.202.1	EXC31	96711	-	-	-	0/3	-	-	-	0/3		0.195	-	110	2/3		_	hypothetical sulfatase/ phosphatase
RBCS2A		108283	2.682	1	74	1/3	-	-	-	0/3		-	-	-	0/3		_	RuBisCO small subunit 2
E_GWW.13.47.1	HCI1	115272	0.964 ± 0.094	1	316	3/3	1.995 ± 0.679	2.069	765	3/3	*	1.361 ± 0.733	1.412	960	3/3		S	hypothetical protein, high similarity to NSG1(nitrogen-starved gametogenesis) protein [PMID: 15459796]
E_GWW.45.64.1	EXC4	121371	0.576	1	80	1/3	-	-	-	0/3		-	-	-	0/3		_	putative translational inhibitor protein
HRP3		127246	-	-	-	0/3	-	-	-	0/3		0.115	-	54	1/3		S	extracellular matrix protein (cell wall protein); contains hydroxyproline-rich domain with (SP)n repeats [PMID: 17932292]
CAH1/CAH2		24120; 128726	1.366 ± 0.179	1	209	3/3	0.537	0.393	82	2/3		0.597 ± 0.198	0.437	100	3/3		S	Carbonic anhydrase1(CAH1); Carbonic anhydrase 2 (CAH2), high-CO2-inducible [PMID: 2124702]
GAP3		129019	4.952 ± 3.225	1	581	3/3	0.992 ± 1.075	0.200	316	3/3		0.944 ± 0.163	0.191	422	3/3		C	Glyceraldehyde 3-phosphate dehydrogenase A
DPA1		129557	0.244	1	58	1/3	-	-	-	0/3		-	-	-	0/3		C	Putative LL-diaminopimelate aminotransferase [PMID: 16361515]
RPL13		129809	1.031	1	122	2/3	0.980	0.951	100	1/3		0.681	0.660	101	2/3		_	Cytosolic 80S ribosomal protein L13; Cytosolic 60S large ribosomal subunit protein L13
TUB2		129868	0.717	1	221	2/3	-	-	-	0/3		-	-	-	0/3		_	Beta-tubulin 2
FEA1	H43/FEA1	129929	6.042 ± 5.501	1	1161	3/3	22.085 ± 8.162	3.655	1826	3/3	*	26.013 ± 4.299	4.305	3020	3/3	*	S	high-CO2 inducible, iron-deficiency inducible, periplasmic protein [PMID: 17660359]; Also known as H43[PMID: 17202179]
EEF1		132905	0.960	1	233	2/3	-	-	-	0/3		0.105	0.109	118	2/3		_	Flagellar Associated Protein, found in the flagellar proteome [PMID: 15998802]
ATPC		134235	-	-	-	0/3	-	-	-	0/3		0.172	-	72	1/3		C	ATP synthase gamma chain
RPE1		135614	0.397	1	58	1/3	0.817	2.059	71	1/3		-	-	-	0/3		C	ribulose phosphate-3-epimerase
LCIC		135713	0.241	1	85	1/3	-	-	-	0/3		-	-	-	0/3		C	low-CO2 inducible protein; homologous to LCIB. Regulated by CCM1 [PMID: 15235119]
CHLRE2_KG.SCAFFOLD_10000228	HCI6	144348	-	-	-	0/3	0.423	-	149	2/3		0.460 ± 0.141	-	191	3/3	*	S	Hypothetical protein, partial sequence similar to Chlamydomonas GAS31[PMID: 16183845] and Pherophorin[PMID: 16367971]
CHLRE2_KG.SCAFFOLD_13000036	EXC11	145123	0.361	1	89	1/3	0.411 ± 0.171	1.137	180	3/3		0.607	1.680	296	2/3		S	Predicted protein, high similarity to pherophorin-C20(Chlamydomonas)[PMID: 16367971]
RPL18A		146844	-	-	-	0/3	-	-	-	0/3		0.670	-	57	1/3		_	Cytosolic 80S ribosomal protein L18a; Cytosolic 60S large ribosomal subunit protein L18a
PHC15		148333	0.397	1	65	1/3	0.676 ± 0.209	1.700	167	3/3		1.536 ± 0.869	3.865	256	3/3		S	Pherophorin-C15 (PHC15) [PMID: 16367971]; belongs to the large pherophorin-family
CHLRE2_KG.SCAFFOLD_23000129	EXC12	148979	-	-	-	0/3	0.724	-	233	2/3		0.344	-	201	2/3		_	Predicted protein, high similarity to matrix Metalloprotease [PMID: 11891059]
CHLRE2_KG.SCAFFOLD_33000129	HCI8	151261	-	-	-	0/3	0.646 ± 0.062	-	69	3/3	*	0.801	-	89	2/3		C	hypothetical protein, partial similarity to pherophorin-C14 [PMID: 16367971]
CHLRE2_KG.SCAFFOLD_46000054	EXC2	152521	3.491 ± 2.042	1	179	3/3	4.923 ± 0.621	1.410	251	3/3		4.438	1.271	225	2/3		C	No domain
CHLRE2_KG.SCAFFOLD_46000056	EXC13	152523	-	-	-	0/3	-	-	-	0/3		0.230	-	76	1/3		_	No domain
METE		154307	0.360	1	279	2/3	0.087	0.241	92	1/3		0.212	0.588	372	2/3		_	5-methyltetrahydropteroyltriglutamate-homocysteine S-methyltransferase
ACEGS_KG.SCAFFOLD_22000039	HCI4	157979	-	-	-	0/3	0.812	-	91	2/3		0.959 ± 0.593	-	79	3/3	*	C	Predicted protein, similarity to GP3 [CAJ98661]
AGG2		159623	-	-	-	0/3	0.359	-	61	1/3		0.284	-	61	2/3		_	Membrane protein required for phototactic orientation [PMID: 16753570]
PGM1B		161085	0.183	1	53	1/3	-	-	-	0/3		-	-	-	0/3		_	Phosphoglycerate mutase
RPP0		164097	-	-	-	0/3	0.200	-	57	1/3		-	-	-	0/3		_	Cytosolic 80S acidic ribosomal protein P0; Cytosolic 60S large ribosomal subunit protein P0
PHC17		164137	0.392	1	58	1/3	0.543 ± 0.268	1.386	83	3/3		0.956	2.441	181	2/3		_	pherophorin-C17 (PHC17) [PMID: 16367971]; belongs to the large pherophorin-family
RPL30		166012	2.623	1	58	1/3	-	-	-	0/3		0.408	0.156	54	1/3		_	Cytosolic 80S ribosomal protein L30; Cytosolic 60S large ribosomal subunit protein L30
FGENESH2_PG.C_SCAFFOLD_7000186	EXC3	166267	0.725 ± 0.163	1	172	3/3	0.820 ± 0.127	1.131	179	3/3		0.592	0.817	143	2/3		S	Hypothetical protein containing a DUF3707; pherophorin domain
FGENESH2_PG.C_SCAFFOLD_3000280	EXC21	167270	-	-	-	0/3	-	-	-	0/3		0.309	-	342	1/3		C	No domain
SRR16		168182	0.044 ± 0.015	1	181	3/3	0.045 ± 0.008	1.040	200	3/3		0.049 ± 0.022	1.120	246	3/3		S	Hypothetical scavenger receptor cysteine-rich protein [PMID: 17932292]
FGENESH2_PG.C_SCAFFOLD_9000253	EXC23	169114	0.214	1	52	1/3	-	-	-	0/3		-	-	-	0/3		_	Selenium-binding protein
FGENESH2_PG.C_SCAFFOLD_1000950	EXC22	172329	0.090	1	68	1/3	0.096 ± 0.027	1.060	140	3/3		0.097 ± 0.018	1.069	164	3/3		_	No domain
FGENESH2_PG.C_SCAFFOLD_19000009	EXC30	172610	0.099	1	93	1/3	0.108 ± 0.061	1.083	272	3/3		0.113 ± 0.053	1.137	368	3/3		S	Predicted protein, partial sequence similar to extracellular matrix protein (cell wall protein) pherophorin-V1 [PMID: 16367971]
FGENESH2_PG.C_SCAFFOLD_19000204	EXC29	172805	0.215 ± 0.048	1	131	3/3	0.157 ± 0.015	0.730	195	3/3		0.125	0.580	136	2/3		_	Predicted flagella associated protein, partial sequence similar to NSG1[PMID: 15459796]
FEA2		173281	0.397	1	57	1/3	-	-	-	0/3		-	-	-	0/3		S	iron-deficiency inducible periplasmic protein [PMID: 17660359]
FGENESH2_PG.C_SCAFFOLD_27000199	EXC27	175296	0.153	1	69	1/3	0.208	1.360	83	1/3		0.189	1.238	81	1/3		S	Hypothetical Leucine-rich repeat family protein
FGENESH2_PG.C_SCAFFOLD_30000041	EXC24	175363	1.100	1	306	2/3	0.672 ± 0.118	0.611	407	3/3		0.556 ± 0.110	0.505	458	3/3		M	hypothetical protein, partial sequence similar to Chlamydomonas GAS31[PMID: 16183845] and Pherophorin[PMID: 16367971]
FGENESH2_PG.C_SCAFFOLD_34000102	EXC25	175796	-	-	-	0/3	-	-	-	0/3		0.349	-	85	1/3		S	Predicted protein, partial sequence similar to extracellular matrix protein (cell wall protein) pherophorin-V1 [PMID: 16367971]
FGENESH2_PG.C_SCAFFOLD_33000142	HCI7	176728	-	-	-	0/3	0.670 ± 0.287	-	160	3/3	*	0.296	-	80	2/3		_	Predicted protein, high similarity to pherophorin-C20(Chlamydomonas)[PMID: 16367971]
FGENESH2_PG.C_SCAFFOLD_33000144	EXC28	176730	-	-	-	0/3	0.386	-	138	2/3		0.140	-	74	2/3		S	Hypothetical protein, partial sequence similar to Chlamydomonas GAS28[PMID: 16183845] and Pherophorin[PMID: 16367972]
FGENESH2_PG.C_SCAFFOLD_39000092	HCI5	177142	-	-	-	0/3	-	-	-	0/3		0.048 ± 0.009	-	75	3/3	*	M	mastigoneme-like flagellar protein
ISG-C1		178049	0.565 ± 0.153	1	232	3/3	2.019 ± 0.444	3.574	639	3/3	*	2.461 ± 0.702	4.357	856	3/3	*	S	Protein similar to Volvox ISG [PMID: 1600938] and Chlamydomonas VSP-3 [PMID: 8000007]; Also known as FAP40 [PMID: 15998802]
FGENESH2_PG.C_SCAFFOLD_81000021	EXC26	180172	-	-	-	0/3	-	-	-	0/3		0.319	-	69	1/3		_	Nucleoside diphosphate kinase
FSD1		182933	1.321 ± 0.301	1	167	3/3	0.604	0.458	110	2/3		0.191	0.145	81	1/3		C	superoxide dismutase [Fe]
RPL6		183518	1.038	1	58	1/3	-	-	-	0/3		-	-	-	0/3		_	Cytosolic 80S ribosomal protein L6; Cytosolic 60S large ribosomal subunit protein L6
ESTEXT_FGENESH2_KG.C_10196	EXC5	183696	-	-	-	0/3	-	-	-	0/3		0.931	-	77	1/3		S	Predicted protein, partial sequence similar to allene oxcide cuclase [PMID: 18937034]
PHOT		183965	0.134 ± 0.030	1	145	3/3	0.098 ± 0.009	0.730	139	3/3		0.081 ± 0.015	0.600	180	3/3		_	phototropin-like, blue light receptor [PMID: 12121468] Found in the flagellar proteome [PMID: 15998802]
ISG-C4		185383	-	-	-	0/3	1.513 ± 0.621	-	152	3/3	*	1.467 ± 0.236	-	187	3/3	*	S	Protein similar to Volvox ISG [PMID: 1600938] and Chlamydomonas VSP-3 [PMID: 8000007]; Also known as FAP137 [PMID: 15998802]
PCY1		185915	1.679 ± 1.231	1	148	3/3	0.717 ± 0.347	0.427	98	3/3		1.191 ± 0.500	0.709	116	3/3		M	pre-apoplastocyanin, PETE [PMID: 2165059;PMID: 8940133]
ESTEXT_FGENESH2_PG.C_70095	EXC7	186470	0.265	1	149	2/3	0.450 ± 0.355	1.701	356	3/3		0.254 ± 0.198	0.959	311	3/3		S	Hypothetical protein containing two DUF3707; pherophorin domains
FAP211		186474	1.903 ± 0.951	1	681	3/3	2.322 ± 1.348	1.220	933	3/3		1.507 ± 0.235	0.792	869	3/3		S	FAP211 [PMID: 15998802], partial sequence similar to NSG1[PMID: 15459796]
ESTEXT_FGENESH2_PG.C_70104	HCI3	186476	0.996 ± 0.372	1	467	3/3	3.434 ± 3.088	3.448	796	3/3		3.016 ± 1.521	3.029	858	3/3	*	_	Predicted protein, similar to flagella associated protein; NSG1protein [PMID: 15459796]
FAP212		186478	0.898 ± 0.021	1	560	3/3	1.566 ± 0.665	1.744	712	3/3		1.658 ± 0.337	1.846	944	3/3	*	S	FAP212 [PMID: 15998802], partial sequence similar to NSG1[PMID: 15459796]
AST3		186959	0.202	1	57	2/3	-	-	-	0/3		-	-	-	0/3		M	Putative aspartate aminotransferase [PMID: 17932292]
ESTEXT_FGENESH2_PG.C_30080	EXC8	187032	0.179	1	77	1/3	0.221 ± 0.145	1.237	131	3/3		0.165	0.925	96	1/3		S	Hypothetical protein containing four DUF3707; pherophorin domains
PHC14		187643	-	-	-	0/3	0.649 ± 0.434	-	241	3/3	*	0.689	-	252	2/3		S	pherophorin-C14 (PHC14) [PMID: 16367971]; belongs to the large pherophorin-family
UPTG1		187866	0.271	1	53	1/3	-	-	-	0/3		-	-	-	0/3		_	could be involved in initiation of starch granule formation [PMID:8521968]
ESTEXT_FGENESH2_PG.C_20105	EXC6	187884	0.517	1	56	1/3	-	-	-	0/3		0.447	0.864	56	1/3		C	Histone H2A
RPS4		188837	0.397	1	52	1/3	-	-	-	0/3		0.166	0.418	52	1/3		_	Cytosolic 40S small ribosomal subunit protein S4
ESTEXT_FGENESH2_PG.C_130125	EXC15	189051	0.179	1	70	1/3	-	-	-	0/3		0.140	0.784	90	2/3		S	Predicted protein, partial sequence similar to Chlamydomonas GAS31[PMID: 16183845] and Pherophorin[PMID: 16367971]
SEBP1		189186	1.155 ± 0.759	1	197	3/3	0.726	0.629	134	1/3		0.510	0.442	155	1/3		C	Sedoheptulose-1,7-bisphosphatase
ESTEXT_FGENESH2_PG.C_10438	EXC9	189937	1.033	1	144	2/3	-	-	-	0/3		-	-	-	0/3		S	Predicted protein, putative desiccation-associated protein [PMID: 19370165]
ESTEXT_FGENESH2_PG.C_180035	EXC10	190273	-	-	-	0/3	0.853	-	67	1/3		0.807	-	74	1/3		_	ribosomal protein L7, component of cytosolic 80S ribosome and 60S large subunit
ESTEXT_FGENESH2_PG.C_180120	EXC19	190320	0.378	1	50	1/3	-	-	-	0/3		-	-	-	0/3		S	Hypothetical protein containing a CHRD (after SWISS-PROT abbreviation for chordin) domain
FAP278		190547	0.336	1	59	1/3	-	-	-	0/3		0.165	0.490	71	2/3		_	No domain
ESTEXT_FGENESH2_PG.C_170153	HCI9	190701	-	-	-	0/3	-	-	-	0/3		0.064 ± 0.012	-	66	3/3	*	S	Predicted protein, partial sequence similar to gametolysin-like matrix metalloproteinase [PMID: 17932292]
ESTEXT_FGENESH2_PG.C_200092	HCI2	190800	1.747 ± 0.756	1	311	3/3	3.363 ± 0.793	1.925	509	3/3	*	2.456 ± 0.272	1.406	472	3/3		_	Predicted protein, similar to flagella associated protein; NSG1protein [PMID: 15459796]
FAP233		191010	0.435	1	195	2/3	0.472	1.085	547	1/3		0.419 ± 0.077	0.962	788	3/3		S	FAP233 [PMID: 15998802], same as GP3 [CAJ98661]
FAP102		191022	1.402 ± 1.143	1	574	3/3	3.165 ± 0.405	2.258	1633	3/3	*	3.481 ± 0.630	2.483	1847	3/3	*	S	FAP102 [PMID: 15998802], high similarity to GP3 [CAJ98661]
ESTEXT_FGENESH2_PG.C_240136	EXC20	191283	-	-	-	0/3	0.391	-	67	1/3		-	-	-	0/3		_	No domain
ESTEXT_FGENESH2_PG.C_230145	EXC1	191447	5.372 ± 2.589	1	497	3/3	4.772 ± 1.390	0.888	415	3/3		3.761 ± 2.612	0.700	736	3/3		S	No domain
RPS5		191776	0.549	1	62	1/3	-	-	-	0/3		0.230	0.418	78	1/3		_	Cytosolic 80S ribosomal protein S5; Cytosolic 40S small ribosomal subunit protein S5
ESTEXT_FGENESH2_PG.C_250053	HCI10	191824	-	-	-	0/3	0.235 ± 0.023	-	200	3/3	*	0.235 ± 0.051	-	232	3/3	*	S	Flagellar associated protein, adenosine kinase-like protein
ARG1		191987	0.275	1	53	1/3	-	-	-	0/3		-	-	-	0/3		C	N-acetyl-gamma-glutamyl-phosphate reductase
CSE1		192228	-	-	-	0/3	-	-	-	0/3		0.069	-	73	1/3		_	Predicted protein, partial sequence similar to NSG1[PMID: 15459796]
ESTEXT_FGENESH2_PG.C_360112	EXC16	192778	0.081 ± 0.018	1	103	3/3	0.059 ± 0.006	0.730	87	3/3		0.047	0.580	89	2/3		_	No domain
GOX18		192937	0.125	1	123	2/3	0.098 ± 0.009	0.784	166	3/3		0.081 ± 0.015	0.644	103	3/3		_	glyoxal or galactose oxidase
FAS7		192980	-	-	-	0/3	-	-	-	0/3		0.047	-	70	2/3		S	Fasciclin(/beta-lg-H3)-like protein [PMID: 17932292],
ESTEXT_FGENESH2_PG.C_430042	EXC17	193449	-	-	-	0/3	-	-	-	0/3		0.038	-	85	1/3		_	Galactose oxidase
ISG-C2		193727	-	-	-	0/3	1.364	-	223	2/3		2.269 ± 0.749	-	316	3/3	*	S	Protein similar to Volvox ISG [PMID: 1600938] and Chlamydomonas VSP-3 [PMID: 8000007]
GAS31		193780	1.072 ± 0.923	1	436	3/3	1.411 ± 0.793	1.316	535	3/3		1.927 ± 0.523	1.798	636	3/3		S	GAS31[PMID: 16183845], belongs to the large pherophorin-family
ESTEXT_FGENESH2_PG.C_540035	HCI11	193961	-	-	-	0/3	0.148	-	114	2/3		0.129 ± 0.024	-	103	3/3	*	M	Protein similar to Volvox ISG [PMID: 1600938] and Chlamydomonas VSP-3 [PMID: 8000007]
AGT1		194541	0.519	1	114	1/3	-	-	-	0/3		-	-	-	0/3		_	putative alanine-glyoxylate transaminase [PMID: 17078018]
ESTEXT_FGENESH2_PG.C_740035	EXC14	194736	0.361	1	84	1/3	0.235 ± 0.023	0.650	83	3/3		0.193 ± 0.036	0.535	135	3/3		C	Glycoside hydrolase
FNR1		195553	0.500	1	97	2/3	-	-	-	0/3		-	-	-	0/3		C	Ferredoxin-NADP reductase
RPL11		195587	-	-	-	0/3	-	-	-	0/3		0.296	-	70	2/3		_	Cytosolic 80S ribosomal protein L11; Cytosolic 60S large ribosomal subunit protein L11
RPS20		195592	-	-	-	0/3	-	-	-	0/3		0.855	-	84	1/3		_	Cytosolic 80S ribosomal protein S20; Cytosolic 40S small ribosomal subunit protein S20
PRPL24		195622	0.417	1	61	1/3	0.381	0.914	52	1/3		0.268	0.642	52	1/3		C	Chloroplast ribosomal protein L24, imported to chloroplast; Chloroplast large ribosomal subunit protein L24
PRPS16		195629	-	-	-	0/3	-	-	-	0/3		0.345	-	56	1/3		C	Chloroplast ribosomal protein S16
GP2		195768	1.791 ± 0.628	1	1587	3/3	2.865 ± 0.787	1.600	3194	3/3		2.359 ± 0.495	1.317	4032	3/3		S	GP2[CAL91937], hydroxyproline-rich glycoprotein [PMID: 1699225]
RB60		195895	0.183	1	79	1/3	-	-	-	0/3		-	-	-	0/3		Endosome	Protein disulfide isomerase 1 (CrPDI1 [PMID: 16143836]
LEU3A		195905	0.364	1	155	2/3	-	-	-	0/3		-	-	-	0/3		C	3-Isopropylmalate dehydrogenase
PHC10		196024	0.329 ± 0.165	1	121	3/3	0.181 ± 0.073	0.550	86	3/3		0.089	0.271	69	1/3		S	pherophorin-C10 (PHC10) [PMID: 16367971]; belongs to the large pherophorin-family
PHC24		196025	0.551	1	65	2/3	0.568	1.032	63	2/3		-	-	-	0/3		_	pherophorin-C24 (PHC24) [PMID: 16367971]; belongs to the large pherophorin-family
PHC13		196029	1.521	1	474	2/3	2.750	1.808	606	2/3		1.202	0.791	303	1/3		S	pherophorin-C13 (PHC13) [PMID: 16367971]; belongs to the large pherophorin-family
CTR3		196115	-	-	-	0/3	-	-	-	0/3		0.064	-	68	1/3		Endosome	copper transport related; high similarity to CTR2 [PMID: 17932292]
CYN19-2		196289	0.914	1	86	1/3	-	-	-	0/3		-	-	-	0/3		_	Peptidyl-prolyl cis-trans isomerase (rotamase) [PMID: 15051864,PMID:15047905]
PHC1		196399	1.938	1	304	2/3	0.950 ± 0.360	0.490	173	3/3		1.573	0.811	282	2/3		S	pherophorin-C1 (PHC1) [PMID: 16367971; belongs to the large pherophorin-family
PHC2		196402	3.223	1	474	1/3	2.585	0.802	666	1/3		2.867	0.890	931	2/3		S	pherophorin-C2 (PHC2) [PMID: 16367971], belongs to the large pherophorin-family
PHC3		196403	0.456	1	129	2/3	0.697 ± 0.264	1.529	262	3/3		0.682 ± 0.206	1.496	403	3/3		S	pherophorin-C3 (PHC3) [PMID: 16367971], belongs to the large pherophorin-family
PHC4		196405	0.761 ± 0.377	1	178	3/3	0.657 ± 0.221	0.863	216	3/3		0.400 ± 0.117	0.526	205	3/3		S	pherophorin-C4 (PHC4) [PMID: 16367971; belongs to the large pherophorin-family
LCI5		196466	1.374 ± 0.915	1	111	3/3	-	-	-	0/3		0.275	0.200	60	1/3		C	low-CO2-inducible protein, regulated by CCM1 [PMID: 15235119]

*: Protein content was significantly ($p<0.05$) higher than that of Air